Università degli Studi di Palermo

AREA QUALITÀ, PROGRAMMAZIONE E SUPPORTO STRATEGICO
SETTORE STRATEGIA PER LA RICERCA
U. O. DOTTORATI




Dottorato in Oncologia e Chirurgia Sperimentali
Dipartimento di Discipline Chirurgiche, Oncologiche e Stomatologiche
MED/06-Oncologia Medica

# POTENTIAL APPLICATIONS OF LIQUID BIOPSY IN IMMUNOTHERAPY: ROLE OF EXOSOMES, MICRORNAS AND PLASMA EXPRESSION LEVELS OF IMMUNE CHECKPOINTS IN PATIENTS WITH SOLID TUMORS

IL DOTTORE
**Chiara Brando**

IL COORDINATORE
**Prof. Antonio Russo**

IL TUTOR
**Prof. Antonio Russo**

EVENTUALE CO TUTOR
**Prof.ssa Lorena Incorvaia**

CICLO XXXV
ANNO CONSEGUIMENTO TITOLO 2023

**Sommario**

# 1. Introduction

Tumours are complex ecosystems composed of neoplastic cells, extracellular matrix (ECM) and non-neoplastic 'accessory' cells, which include mesenchymal cells, endothelial cells and infiltrating inflammatory immune cells.

The interaction between tumour cells and accessory cells drives and influences tumour development and leads to functional and compositional changes in the immune system (1). Crosstalk between tumour cells and stromal cells significantly determines tumour heterogeneity and antitumour immunity. Through continuous dynamic interactions, immune system cells, on the one hand, transmit protective anti-tumour immunity by destroying immunogenic tumour variants and, on the other hand, promote tumour progression by modelling its immunogenicity. This dynamic process, termed 'cancer immunoediting', suggests the dual role of the immune system in inhibition or promotion of tumour, integrates the complex interactions between immune system and tumour cells within the tumour microenvironment, modulates immunogenicity and antigenicity, and is associated with tumour evasion from immune surveillance (2). The immunoediting hypothesis encompasses all stages of cancer and is regulated in a complex mechanism that consists of three phases: elimination, equilibrium and escape (3) (**Figure 1**).

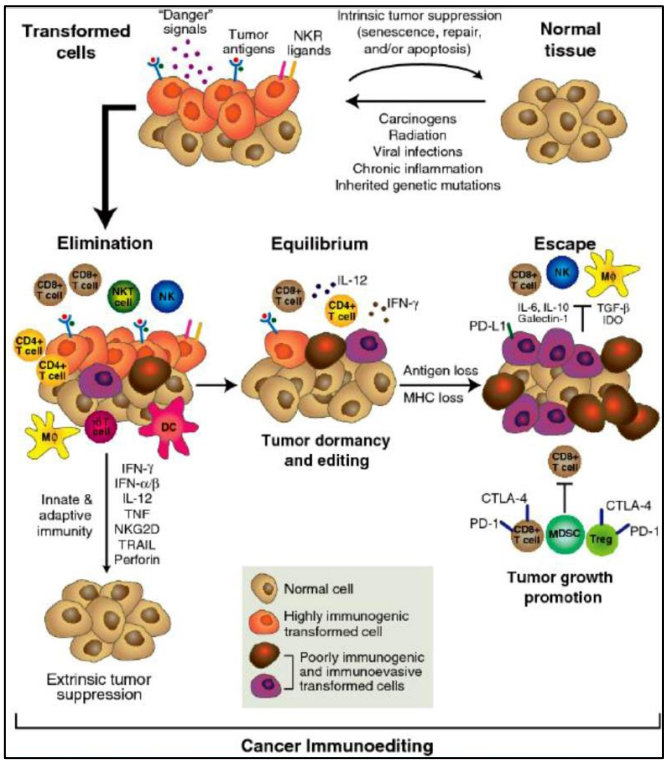


**Figure 1**: Cancer Immunoediting (4).

The first phase of immunoediting is the elimination and it represents the time when immunosurveillance is active. Cells, which are not repaired by intrinsic genetic DNA repair mechanisms, become malignant or potentially malignant and can be initially detected and eliminated by innate and adaptive immune systems through immunosurveillance. Innate immunity is followed by adaptive immunity which, through presentation to tumour antigens and dendritic cells, leads to the development of tumour-specific CD4+ and CD8+ T cells that allow tumour cell destruction (4). If the developing tumour is destroyed, elimination is the end point of immunoediting. However, if the tumour cells are not eliminated, they initially enter a state of equilibrium with the immune system, the second stage of immunoediting. In the equilibrium phase, the immune system controls tumour growth and the tumour cells, which are unable to progress, enter a dormant state and continue to coexist with the immune system (3). The third phase of immunoediting is escape or evasion. During the escape phase, tumour cells, which have escaped the control of the immune system, begin to grow and proliferate uncontrollably, leading to clinically evident tumours (4).

In order to escape the immune system's control, cancer cells use different mechanisms, including some of the normal immune response control circuits called immune checkpoints (ICs) that, under physiological conditions, degrade the activation of T lymphocytes and their effector functions (4).

T-cell activation is a key step in initiating and regulating the immune response that requires co-stimulation with "two signals" from antigen presenting cells (APCs). The first signal or "antigen-specific signal" is the binding of the antigen presenting the major histocompatibility complex (MHC) to the T-cell receptor (TCR). If T cells receive only antigen-specific TCR stimulation they will become unresponsive to subsequent antigenic challenge (5). The second signal consists of co-stimulatory and co-inhibitory signals to T cells (5). Among co-inhibitory stimuli, IC proteins provide co-inhibitory signals to negatively modulate T-cell activation, contributing to poor anti-tumor T-cell efficacy (5).

ICs are co-inhibitory signaling pathway molecules that act to maintain immune tolerance, but are often used by cancer cells to evade immunosurveillance.

The programmed cell death protein-1/programmed cell death-ligand 1 (PD-1/PD-L1) axis is a vital IC signalling pathway that controls the induction and maintenance of immune tolerance in the tumour microenvironment and maintains immune homeostasis (6).

Physiologically, ICs maintain self-tolerance and regulate physiological immune balance by protecting healthy tissues from immune system attack. When activated following a stimulus, T cells express PD-1 which allows them to recognize abnormal and cancerous cells. Conversely, in order to evade recognition and elimination by T cells, cancer cells express PD-L1 which binds PD-1 on T cells, rendering them inactive (6). Activation of this pathway can lead to tumour immune escape and

promote tumour cell growth, as well as cause T-cell depletion and apoptosis and enhancement of immunosuppressive Treg cell function (6). (**Figure 2**)

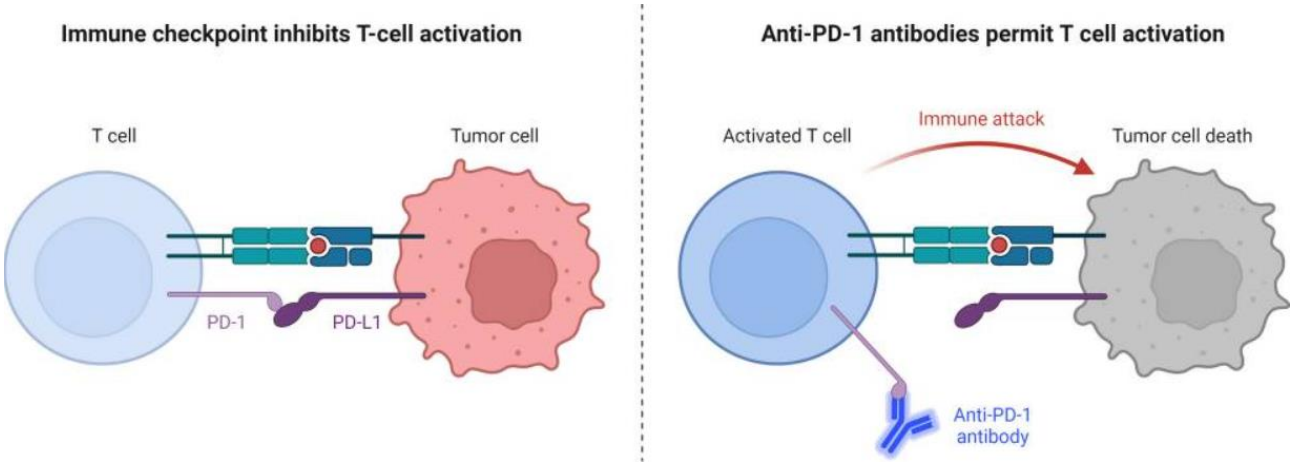


**Figure 2**: Immune checkpoint inhibitor against cancer cells. Through the interaction between PD-1 expressed on the surface of T cells and PD-L1 expressed on the surface of tumor cells, the immunological checkpoint prevents the activation of T cells. Through the contact between PD-1 on the surface of T cells and the anti-PD-1 antibodies, T cell activation and immunological attack are enabled (7)

Both PD-1 and PD-L1 are type I transmembrane proteins that belong to the immunoglobulin (Ig) superfamily.

PD-1 is a transmembrane protein expressed on activated T lymphocytes, natural killer (NK) and B cells, macrophages, dendritic cells (DC), regulatory T cells (Tregs) and monocytes. It contains one Ig-V like extracellular domain, a transmembrane domain, and a cytoplasmic domain with two tyrosine signaling motifs. PD-1 expression can be induced by T-cell receptor (TCR)-mediated activation and stimulation by cytokines such as interleukin (IL)-2, IL-7, IL-15 and IL-21. In many types of cancers, it is expressed on a large proportion of tumor infiltrating lymphocytes (TILs). PD-1 has two ligands, PD-L1 and PD-L2, and although the interaction with PD-L2 shows higher affinity, PD-L1 is considered the main ligand of PD-1 (8).

PD-L1 is an inhibitory receptor expressed on the surface of tumor cells and it is commonly upregulated in tumor cells. It contains two extracellular domains (Ig-V- and Ig-C-like), a transmembrane domain, and a short cytoplasmic tail which lacks known signaling motifs. In cancer cells PD-L1 acts as a pro-tumorigenic factor by binding to its receptors and activating proliferative and survival signaling pathways (9). It can be expressed constitutively or as a mechanism of resistance (9). Oncogenic signals, such as PI3K-AKT, MEK-ERK, and EGFR (10-12), as well as several cytokines, such as IL-4, IL-6, IL-10 and IFN-γ (13, 14), have been found to regulate PD-L1 expression (15).

PD-1 limits the functional activation of cytotoxic T lymphocytes and it can induce apoptosis and promote the differentiation of CD4+ lymphocytes into Treg. The PD-L1 ligand is usually expressed by tumour cells, macrophages, some activated T-cells and B-cells, DC (9). High expression of PD-L1 on tumour cell causes T-cell depletion, thus attenuating tumour-specific immunity that promotes tumour progression (6).

Interaction between PD-1 on T cells and PD-L1 on tumor cells or APC inhibits T cell activation and its cytolytic effector functions. Overexpression of PD-L1 on tumor cells leads to the formation of an immunosuppressive microenvironment that facilitates cancer evasion from the immune system through downregulation of cytotoxic T cell activity (6).

The mechanism by which PD-1 exerts its inhibitory effect has been partially elucidated. Following the interaction between PD-L1 and PD-1, phosphatase-1 (SHP-1) and SHP-2 containing the Src homology region domain 2 are recruited, which dephosphorylate multiple members of the TCR signaling pathway. Dephosphorylation nullifies the downstream effects of T cell activation, including cytokine production, cell cycle progression, and survival protein expression (16).

Inhibition of PD-1 or PD-L1 could restore the cytotoxic capacity of T-cells and induce tumour regression, suggesting that use of immune checkpoint inhibitors (ICIs) could serve as therapeutic targets (17).

The introduction of ICIs into clinical practice has become a promising frontier of immuno-oncology that has achieved surprising therapeutic effects in a variety of cancers. ICIs aim to reinvigorate anti-tumor immune responses by disrupting co-inhibitory signaling pathways and promoting immune-mediated elimination of malignant cells (17).

The first immunotherapy drug approved for the treatment of patients with metastatic melanoma was Ipilimumab, in 2011, a protein that blocks CTLA-4, a key inhibitory control molecule that counter acts the co-stimulatory signal of CD28, competitively binding to its ligands (B7.1 and B7.2) on the surface of cells presenting the antigen (18). In the United States, the FDA has approved Nivolumab, Pembrolizumab, and Cemiplimab as PD-1 inhibitors and Atezolimumab, Durvalumab, and Avelumab as PD-L1 inhibitors for the treatment of several solid tumors, including non-small cell lung cancer (NSCLC), melanoma, urothelial carcinoma, head and neck squamous cell carcinoma (HNSCC) and Merkel cell carcinoma (MCC) (19).

Immunotherapy, through the use of monoclonal antibodies that bind directly to PD-1 or PD-L1 has radically revolutionized the therapeutic approach of cancer by shifting the therapeutic target from the neoplastic cell to the T lymphocyte (20). Blockade of the PD1/PD-L1 axis with specific antibody inhibitors prevents T-cell suppression and promotes immune killing of tumor cells (20).

PD-1/PD-L1 ICIs have been widely used in the treatment of different cancers (21-23) becoming a promising frontier for the treatment of numerous solid tumors, such as non-small cell lung cancer (NSCLC), melanoma (24-28), renal cell carcinoma (RCC) (29), but also small cell lung carcinoma (SCLC) (30) and breast (31), neck (32), bladder (33-35), colorectal (36), stomach (37) and liver (38). Despite the efficacy of PD-1/PD-L1 ICIs and the marked improvement in patient outcome, durable responses are observed in only a minority of patients and the phenomena of primary and acquired resistance to therapy, treatment-related adverse effects and the lack of predictive biomarkers are still numerous (39).

In primary resistance patients do not show a clinical response or stable disease during treatment with PD-1/PD-L1 ICIs, due to lack of tumor immunogenicity (40), immunosuppressive factors in the tumor microenvironment (41), lack of response to interferon (42), epidermal growth factor receptor (EGFR) mutations, and anaplastic lymphoma kinase (ALK) rearrangements (43). In cases of acquired resistance, on the other hand, patients show effective and lasting responses only at the beginning of the treatment, which subsequently decrease or disappear completely. The mechanisms underlying acquired resistance may be related to tumor microenvironment complexity (44), lack of memory T cells (45), loss of T cell function (46-48), and upregulation of other ICs (49).

Furthermore, identifying predictive biomarkers predicting which patient will benefit from ICIs is a novel and important issue and would contribute to optimize treatment selection (6).

The use of PD-1/PD-L1 as the only predictive biomarker for cancer immunotherapy still remains problematic.

Until now, the only predictive biomarker used as a complementary diagnostic test for first-line immunotherapy is PD-L1 expression assessed by Immunohistochemistry (IHC) staining in Formalin-Fixed, Paraffin-Embedded (FFPE) from tissue sections (50). PD-L1 expression has been shown to be a potential predictive biomarker for response and outcome of anti-PD-1/PD-L1 immunotherapy (20). In patients with PD-L1 positive tumors (≥ 5% staining for PD-L1 on tumor cells) the ORR was 36% (9 of 25 patients) whereas in patients with PD-L1 negative tumors there was no objective clinical response observed (0 of 17 patients). PD-L1 expression on cancer cells has a high predictive value in melanoma and NSCLC (51) and predicts worse outcome in cutaneous angiosarcoma (52). Melanoma patients exhibit a response rate of 44%-51% to anti-PD-1-directed therapy while low tissue PD-L1 expression correlates with response rates of around 6%-17%. Similarly, NSCLC patients with IHC PD-L1 overexpression have a response rate of 67%-100% while for PD-L1-negative the response rate was around 0%-15% (53, 54). In gastric cancer exhibiting high microsatellite instability (MSI-H), PD-L1 expression by immune cells is an important marker of overall survival (OS) (55). Phase 1 study of pembrolizumab (KEYNOTE-001) in NSCLC patients showed ORRs (ORR) of 45% and

11% in patients with PD-L1 positive tumors (defined by immunohistochemistry with ≥50% tumor cells) and PD-L1 negative (defined by immunohistochemistry with <1% of tumor cells), respectively (56).

In triple negative breast cancer (TNBC), the KEYNOTE-012 study, which tested pembrolizumab monotherapy in PD-L1 positive metastatic TNBC patients, showed a 20% clinical benefit rate with 1 complete response, 4 partial responses, and 7 cases of stable disease (>10 months) (PMID: 27138582). Also in the Phase 1 study with an anti-PD-L1 antibody, atezolizumab, the ORR was 19% with a variable duration of response (from 0.1 to > 41.6 weeks) (57). Advanced urothelial cancer study showed better survival and fewer side effects in patients treated with pembrolizumab (58). Additionally, results from the KEYNOTE-048 study in patients with recurrent/metastatic HNSCC showed improvement in OS with increasing PD-L1 (59). Significant clinical responses after treatment with anti-PD-L1 antibodies were also found in PD-L1 positive bladder cancer patients with an ORR of 46% (60). Another study evaluating the antitumor activity of avelumab, an anti-PD-L1, in patients with metastatic urothelial bladder cancer showed a PFS of approximately 12 weeks and a median OS of approximately 14 months (61).

However, PD-L1 status on tumor tissue has been shown to be an imperfect predictive biomarker due to numerous biological and technical limitations. The detection of PD-L1 on tumor cells and/or immune cells by IHC still has many limitations due to the complexity related to the different staining performance of immunohistochemical assays, different scoring methods that evaluate various cellular compartments within tumors, and intra- and intertumor heterogeneity (62).

Intratumor heterogeneity represents another obstacle in determining PD-L1 and its predictive value. Samples of tumor tissue can be obtained from surgery, core needle biopsies, and fine needle aspirations, and for most patients, only one sample is taken from a single lesion, even in the presence of multiple metastases (62).

Furthermore, the expression of ICIs on immune and tumor cells is a dynamic process. Indeed, PD-L1 and PD-1 are dynamic molecules and their tissue expression, which changes during disease progression and treatment, may not provide a comprehensive overview of the disease. Thus, PD-L1 status may be underestimated in small biopsies (such as bronchial and transthoracic), which are not representative of the entire tumor (62).

To date, there are only three PD-L1 tests approved by the FDA as "complementary" diagnostic tests and they are Dako 22C3 for pembrolizumab in patients with a variety of solid tumors; Ventana SP142 for atezolizumab in patients with urothelial cancer, triple negative breast cancer (TNBC), or NSCLC; and Dako 28-8 for the combination of ipilimumab and nivolumab in patients with NSCLC (63).

However, PD-L1 expression alone is not sufficient as a predictor for stratification of patients responding to immunotherapy (50).

Other factors may collaborate with PD-L1 as biomarkers to better predict sensitivity to anti-PD-1/PD-L1 inhibitors, including elevated tumor mutational burden (TMB) expression, microsatellite instability (MSI), and lymphocyte infiltration Cytotoxic T (50).

Recently, a link between PD-L1 expression, TMB, and MSI with ICIs response has been reported in several tumor types, including NSCLC and melanoma (64, 65).

More interestingly, the co-occurence of a high TMB and PD-L1 expression level of at least 50% has been suggested as predictor of response to nivolumab in NSCLC since in this subset ORR was 75% compared to 16% in that with neither factor (66).

Furthermore, a considerable immunoregulatory function has been recently demonstrated also for a family of transmembrane glycoproteins, named butyrophilins (BTNs), which are part of the immunoglobulin (Ig) superfamily (67) that have been shown to play a critical role in modulating γδ T-cell development and differentiation (68). Recent clinical studies reported the modified expression of molecules belonging to the BTN/BTNL family following IC blockade with anti-PD-1 antibodies (69, 70), suggesting their unexplored role in tumor immune escape (71).

A putative role of butyrophilins is under investigation as a novel mechanism of cancer immune evasion.

PD-1 or PD-L1 expression can also be regulated by non-coding RNAs such as microRNAs (miRNAs) and long non-coding RNAs (5, 72). miRNAs are small single-stranded non-coding RNAs containing approximately 22 nucleotides playing important roles in the modulation of gene expression. By binding with the 3' non-translational region (3' UTR) of target mRNAs, miRNAs can induce mRNA degradation and translational repression, downregulating the expression of their target genes (5).

Numerous studies suggest the role of miRNAs as tumour suppressors, cancer biomarkers, diagnostic and prognostic in lung cancer (73), as regulators of cancer cell metabolism and in resistance or sensitivity to chemotherapy and radiotherapy (74).

Some miRNAs have been found to target PD-1 or PD-L1 and regulate their expression levels in tumour cells, being implicated in tumour immune escape, leading to the development of microenvironments favourable to tumour growth and progression (5, 9).

For example, miR-28, miR-4717, miR-155, miR-33a, miR-138 and miR-374b modulate PD- 1 expression, whereas miR-570, miR-513, miR-155, miR-140-3p, miR-152, miR-25-93-106b, miR-200 and miR-34 regulate PD-L1 expression (72).

miR-155, overexpressed in some solid tumours, is related to cell growth, invasion, migration, stemness and inhibition of apoptosis (75). Recent data also indicate that miR-155 plays a key role in

the activation of the immune system, as miR-155 inhibition of tumour-related immune cells may promote tumour immune escape and promote tumour growth (76).

miR-34 possesses tumour suppressive properties, such as inhibition of cell migration, invasion, proliferation, survival, EMT and stemness, and drug resistance (77) . A recent study by Cortez et *al*. (78) observed a correlation between overexpression of miR-34b or miR34c and inhibition of PD-L1 protein expression.

Literature data demonstrate the role of miR-33a in the regulation of immune marker expression (79). In the study by Boldrini et *al*. (80) in patients with lung adenocarcinoma, analysis of the association between miR-33a and PD-1/PD-L1 expression levels exhibited a negative correlation and lower levels of miR-33a in patients with higher PD-1, PD-L1 and CTLA4 expression. To investigate the association between patient survival, miR-33a and PD-1, patients were divided according to miR-33a and PD-1 expression, and differences in survival of the two groups (high miR- 33a/low PD-1 expression and low miR-33a/high PD-1 expression) were compared. The first group (patients with high miR-33a and low PD-1 levels) had a better prognosis, suggesting that miR-33a is a good prognostic marker as a result of PD-1 regulation (80).

miR-21 is one of the most abundant miRNAs in mammals, comprises about 10% of total miRNAs in several tumour cell types and it is a critical factor involved in immune responses (9, 81). It was shown that PD-1 is a negative regulator of miR-21 and that PD-1 inhibition increased miR-21 expression, reducing Treg cells and increasing Th17 cells in patients undergoing gastric cancer resection (82).

miRNAs can also indirectly modulate PD-1/PD-L1 expression through their upstream or downstream pathways. For example, miR-197 and miR-3127-5p target STAT3, a regulator of PD-L1 expression, to indirectly modulate PD-L1 levels (83, 84).

miR-21 subregulates JAK2 and STAT1 to inhibit IFN-γ-induced STAT1 signalling. In this way, miR-21 decreases PD-1 expression in macrophages (85). MiR-20b, miR-21 and miR-130b inhibiting phosphatase and PTEN enhance PD-L1 expression (86).

Several components such as proteins, exosomes and other circulating vesicles can be analysed using liquid biopsy (87). Among these, the role of exosomes in the immunomodulatory response is under investigation. Exosomes are biologically active lipid bilayer vesicles about 30-100 nm in size that play an important role in intercellular communication and influence the extracellular environment and the immune system (88). These vesicles, released from different normal or tumour cell types, are secreted into the extracellular space via endosomal pathways and transport various bioactive molecules to target cells. The composition of the exosomal cargo is highly varied and includes a wide range of immunosuppressive and immunostimulatory proteins, chemokines, cytokines, cellular receptors, lipids, as well as various nucleic acids such as micro-RNAs and circular RNAs (88).

Tumour cells can produce and release large levels of exosomes enriched with cellular contents that promote cancer, such as immunosuppressive proteins like PD-L1, mRNAs and micro-RNAs, which participate in cancer development and metastasis, through dysregulation of anti-tumour or pro-tumour immune responses and by promoting drug resistance (89-91). Tumour cells can produce and release large levels of exosomes enriched with cellular contents that promote cancer, such as immunosuppressive proteins like PD-L1, mRNAs and micro-RNAs, which participate in cancer development and metastasis, through dysregulation of anti-tumour or pro-tumour immune responses and by promoting drug resistance (89-91). Several data reveal a significant association between circulating exosomal PD-L1 levels and the response rate to anti-PD-1/PD-L1 antibody therapy (88). Higher concentrations of exosomal PD-L1 prior to anti-PD-1 therapy are associated with a worse prognosis in melanoma patients. This could consequently be a more robust approach than soluble PD-1/PD-L1 levels (92). Tumour-secreted exosomes contain PD-L1 presented either on the surface or within exosomal particles and can transport it to other cells with low or absent PD-L1 expression, with the possibility of binding to PD-1 (93). Plasma/serum levels of PD-L1 expressed on exosomes are associated with tumour progression and clinicopathological features in patients with HNSCC and NSCLC (94), acting as an important biomarker (95). Tumour-derived exosomes containing PD-L1 can reverse the effect of PD-L1 on the cell surface, and are able to induce tumour progression by allowing tumour cells to escape anti-tumour immunity through inhibition of T-cell activation (88). In patients with HNSCC, low or high levels of exosomal PD-L1 suppressed CD4+ T-cell proliferation, induced apoptosis in CD8+ T-cells and enhanced the suppressor activity of Treg cells, depending on the level of PD-L1 in exosomes (94).

Based on this evidence, we investigated the potential role of the levels of sICs, including sPD-1, sPD-L1 and sBTN (pan-sBTN3A, sBTN3A1 and sBTN2A1), microRNAs and exosomes as predictive biomarkers of response to immunotherapy treatment in certain solid tumours.

## 2. Background

The introduction and evolution of immuno-oncology, and in particular of ICIs, has become a promising frontier for treatment of various tumours, strengthening and increasing the capacity of the immune system against the tumour (92).

However, although a clinically relevant median duration of response has been reported, treatment efficacy is variable and poorly predictable in daily clinical practice. Thus, the variability of clinical response to immunotherapy requires the discovery of predictive biomarkers for patient selection.

Although it has been shown that PD-1/PD-L1 expression may have a predictive and prognostic role, the value of assessing PD-L1 expression by IHC staining in paraffin-embedded and formalin-fixed tissue samples is currently debated and challenged. (50). IHC technical methods and biological heterogeneity within the tumor sample represent the major limitation to the use of PD-L1 expression as a predictive biomarker to identify patients likely to benefit from immunotherapy. Furthermore, the expression of ICs on immune and tumor cells is a dynamic process, and PD-L1 expression during cancer evolution and treatment is heterogeneous; therefore, evaluation at a single time point may be suboptimal due to several limitations (92).

Consequently, the current effort is to identify peripheral blood biomarkers that reveal the dynamic and complex nature of the immune response and the interaction of multiple elements and aid in therapeutic decisions in the clinic.

Several components, using the liquid biopsy, are being studied as predictive biomarkers of response or resistance to immunotherapy, such as circulating tumor cells (CTC), cell-free DNA (cfDNA) and exosomes, but also T lymphocytes (the T cell receptor), cytokines, soluble forms of ICs and other circulating proteins (92). Among the various peripheral blood biomarkers studied, the plasma soluble forms of PD-1 and PD-L1 (sPD-1; sPD-L1) represent the areas with the most encouraging data. The prognostic and predictive role of sPD-1 and sPD-L1 appears to depend on the type of tumor, leading to good or bad clinical outcomes (96). sPD-1 and sPD-L1 have been shown to be negatively correlated with survival in NSCLC; clinical outcome of nivolumab treatment was significantly associated with baseline sPD-L1 plasma levels. In patients with metastatic melanoma, the level of circulating exosomal PD-L1 changes during treatment with the anti-PD-1 pembrolizumab. A higher level before treatment has been associated with worse clinical outcomes, while increasing levels during the early stages of therapy identifies clinically responding patients (96).

The prognostic and predictive role of sPD-1 and sPD-L1 appears to depend on tumor type, leading to different clinical response. sPD-1 and sPD-L1 have been shown to negatively correlate with survival in NSCLC. The clinical outcome of nivolumab treatment was significantly associated with baseline plasma sPD-L1 levels (27). In patients with metastatic melanoma, the level of circulating exosomal

PD-L1 changes during treatment with the anti-PD-1 pembrolizumab ; therefore, plasma PD-1 appears to predict the presence and efficiency of tumor-infiltrating lymphocytes in metastatic melanoma (24). Higher levels before treatment are associated with worse clinical outcomes, while higher levels during the early stages of therapy identify clinical responders. Elevated plasma levels of specific ICs have been shown to correlate with dramatically negative outcome and may be used as prognostic factors in unresectable pancreatic adenocarcinoma (PDAC) (97).

A study by Zheng et *al*. (98) demonstrated that adenocarcinoma patients with higher levels of sPD-L1 had a better prognosis than patients with low levels.

In a study of NSCLC patients, approximately 40% of erlotinib-treated patients with elevated sPD-1 levels while on treatment had prolonged progression-free survival (PFS) and OS (OS) compared to patients without elevated sPD-1 (99). NSCLC patients with increased or stable sPD-1 after anti-PD-1 therapy also showed favorable outcomes (100).

In a retrospective study of patients with hepatocellular carcinoma (HCC) undergoing radical resection, a correlation was observed between increases in sPD-1 and longer survival (101).

Conversely, high levels of sPD-1 in untreated cancer patients have been related to poor survival outcomes (102). In general, elevated sPD-L1 levels are indicative of poor prognosis or resistance to treatment (103). Higher levels of sPD-L1 were observed in patients with metastatic than in non-metastatic clear cell renal cell carcinoma (104) and in patients with muscle invasive and metastatic urinary bladder cancer (105).

Elevated pretreatment sPD-L1 concentration may be a marker of poor prognosis in patients with locally advanced or metastatic esophageal squamous cell carcinoma treated with chemotherapy (106). Higher baseline sPD-L1 levels in glioma patients treated with radiotherapy were associated with lower PFS and OS (107), and elevated sPD-L1 levels were considered a biomarker of poor prognosis in HCC patients undergoing curative treatment (108). In melanoma, high pretreatment sPD-L1 was associated with a higher likelihood of disease progression (109). Furthermore, elevated sPD-L1 levels were significantly associated with lower OS and PFS in ICI-treated lung cancer patients (110).

Therefore, the current effort is to identify peripheral blood biomarkers that reveal the dynamic and complex nature of the immune response to correctly select patients who will benefit from immunotherapy. In a new era of liquid biopsy, all of these data are interesting findings that provide a rationale for applying more precise and dynamic predictive biomarkers for checkpoint blockages.

# 3. Patients and methods

## 3.1 Study Population

A prospective study was carried out at the 'Sicilian Regional Center for the Prevention, Diagnosis and Treatment of Rare and Heredo-Familial Tumors' of the Section of Medical Oncology of University Hospital Policlinico 'P. Giaccone' of Palermo.

The study included 4 patient cohorts:

- a cohort of 30 metastatic gastrointestinal cancer (mGIST) patients (cohort number 1);
- a cphort of 56 metastatic clear cell renal cell carcinoma (mccRCC) patients (cohort number 2);
- a cohort of 23 mccRCC patients (cohort number 3);
- a cohort of 41 melanoma patients (cohort number 3).

For all patients enrolled in the study, who provided written informed consent, all clinical information was collected and recorded anonymously.

Clinical and pathological information included gender, age of cancer diagnosis, histological tumor subtype, molecular phenotype and disease stages (I-IV), site of origin of primary tumors, site of active disease, site and number of metastasis, surgery, treatment type, treatment response, tumor response [disease in progression (PD), stable disease (SD), partial response (PR), complete response (CR)] assessed according to response evaluation criteria in solid tumors (RECIST version 1.1.) and progression-free survival (PFS), ORR (ORR), and OS (OS).

Additional clinical data including neutrophil-lymphocyte ratio (NLR) and body mass index (BMI) were collected in melanoma patients in the cohort 3.The NLR was recorded from the routinely performed blood cell count, as the absolute count of neutrophils divided by the absolute count of lymphocytes from peripheral blood samples collected at baseline. BMI was calculated as weight in kilograms divided by height in meters squared. Normal weight (BMI = 18.5–24.9), overweight (BMI = 25–29.9), and obesity (BMI $\geqslant$ 30) were classified based on the World Health Organization recommendations.

The study (Protocol 'G-Land 2017') was approved by ethical committee (Comitato Etico Palermo 1; approval number: 0103-2017) of the University-affiliated Hospital AOUP 'Paolo Giaccone' of Palermo.

## 3.2 Sample Collection and Lymphocytes Isolation

All samples were collected at baseline (T0) before treatment initiation. In the mccRCC patients of cohort number 2 and 3, the sampling was also carried out at 4 weeks (T1), after two drug administration cycles.

The peripheral blood samples, obtained by venipuncture, were processed within 2 h of collection, by centrifugation at 2.200 g for 15 min at 4°C in presence of ethylenediaminetetraacetic acid (EDTA). The isolated supernatants (plasma fractions) were aliquoted in cryotubes and stored at −80°C until their use for subsequent analysis.

After plasma isolation and separation, the 4 blood tubes, to which 3 mL of Lympholyte (Lympholyte-H cell separation media, CL5020, Cederlane) were added, were centrifuged at 800 r.c.f. for 20 min at 18 °C. After centrifugation, a white colored ring containing lymphocytes can be isolated in the interface. The isolated lymphocytes were aliquoted in cryotubes and stored at −80 °C until their use for subsequent analysis.

## 3.3 Determination of soluble ICs concentrations in plasma

The plasma sPD-1, sPD-L1, and pan-sBTN3A, sBTN3A1, and sBTN2A1 levels have been measured using specific homemade enzyme-linked immunosorbent assays (ELISAs) assays not yet commercially available. Because some discrepancies were observed in monitoring the three other proteins when using commercial kits obtained from different sources, we decided to have ELISAs of the 5 markers produced by DYNABIO S.A. (Parc de Luminy, Marseille France) according to our specifications. These specifications included (i) verification by tandem mass spectrometry of the antigen sequence, (ii) optimization of the assay by testing all combinations of available monoclonal antibodies in capture and detection, targeting maximal signal/background ratio and sensitivity. Combinations of two or more antibodies in coating and/or detection were also tested to improve performances, (iii) checking sample compatibility (serum vs plasma, interference of the matrix), (iv) ensure that assay can be run at room temperature for easy handling and robustness. The mAbs were made in D. Olive laboratory immunizing mice with recombinant PD-1, PD-L-1, BTN3A1, BTN3A and BTLA molecules. The hybridomas were screened for the ability to bind to recombinant PD-1, PD-L1, BTN3A1, BTN3A and BTLA molecules. They are all of IgG1 isotype.

All five ELISAs follow the same schedule: All steps are run at room temperature. Plates are coated overnight with the antibody selected for capture then washed. Remaining binding sites are blocked to minimize background. All next steps end with plate washing. For the PD-L1 assay, all steps are conducted under shaking. Samples to be tested are incubated for 3 h. Then, the biotinylated antibody selected for detection is incubated for 30 min, followed by incubation for 15 min with the avidin–peroxidase conjugate. Finally, the substrate TMB is incubated for 15 min, the reaction stopped with H2SO4 and the OD read at 450 nm. Concentrations are established by comparison with a range obtained with known concentrations of the recombinant antigen. All recombinant antigens except PD-L1 (obtained from R&D, cat# 156 B7) were home-synthesized.

The five ELISA tests used showed good linearity and a high specificity. The linearity for sPD-1 measurement in the test ranges from 0.05 to 5.00 ng/mL, for sPD-L1 from 0.02 to 2.00 ng/mL, for sPan-BTN3As from 0.10 to 8.00 ng/mL, for sBTN3A1 from 0.10 to 8.00 ng/mL, and for sBTN2A1 is from 0.06 to 2.00 ng/mL. Also, we tested the cross reactivity between these five recombinant proteins and, as expected, no signal was detected when the antibodies used did not correspond to the antigen.

Studies comparing concentrations of all 5 markers measured in serum and plasma from the same blood collection showed that apparent concentrations in serum were at least three to five times less than in plasma as shown in supplementary Figure 1. This observation shows that clotting results in the apparent loss of a large part of the assayed proteins. Because the mechanism of such loss is unknown, determination of protein concentrations in serum might be affected by factors other than the clinical status of the patient. As consequence, use of serum samples could be misleading and should be avoided. All samples assayed in this study were plasmas. We also observed in all 5 ELISAs an interference of the plasma matrix, which becomes negligible when plasma samples are diluted at least 1/5. In the present study, all plasma samples were at least diluted 1/5 before assay.

Details on the five ELISAs are summarized in Table 1.

**Table 1. Characteristics of ELISAs for sPDL-1, sPD-1, sPan-BTN3A, sBTN3A1 and BTLA.**

| | PD-L1 | PD-1 | Pan-BTN3A* | BTN3A1* | BTLA |
|---|---|---|---|---|---|
| **Coating Ab** | α-PD-L1 1.8 + α PD-L1 2.1 | α-PD-1 6.4 | α-BTN3A S148 | α-BTN3A1 S240 | α-BTLA 75.2 |
| **Detection Ab (biotinylated)** | A-PD-L1 1.3.1 | α-PD-1 3.1 | α-BTN3A 103.2 | α-BTN3A 103.2 | α-BTLA 7.1 + α-BTLA 8.2 |
| **Detection limit (pg/ml)** | 20 | 50 | 100 | 100 | 200 |

*Three isoforms of BTN3A are identified (A1, A2, A3). Among available monoclonal antibodies (Ab) to BTN3A, one is specific for A1 (α-BTN3A1 S240). Coating with α-BTN3A1 S240 allows specific assay of the A1 isoform, whereas the couple of antibodies α-BTN3A S148 and α-BTN3A 103.2 allows simultaneous detection of all three forms (Pan-BTN3A assay). It is however noteworthy that BTN3A concentrations obtained with the Pan-BTN3A assay are only indicative since the range used in the assay is pure BTN3A1. BTN3A concentrations should, therefore, be expressed as pg/ml « equivalent BTN3A1 ».

## 3.4 miRNA Expression Profile Analysis

Total cellular RNA and miRNAs have been isolated using the miRNeasy Mini Kit (Qiagen Inc, Valencia, CA, USA). The quality of the samples have been controlled through RNA 6000 Nano Assay

(Agilent Technologies, Palo Alto, CA, USA) using 2100 Bioanalyzer (Agilent Technologies, Santa Clara, CA, USA) and quantified through the spectrophotometer NanoDrop ND-1000 (CELBIO). To study miRNA expression profile, we used TaqMan® Low Density Array A Human MicroRNA v2.0 (Life Technologies, Carlsbad, CA, USA).

The arrays were processed and analyzed in accordance to manufacturer's protocols.

Briefly, 600 ng of miRNA-enriched total RNA were reverse transcribed using Megaplex™ RT Primers Human Pool A (Life Technologies, Carlsbad, CA, USA) according to manufacturer's instructions. Conditions for the reverse transcription reaction were as follows: 16°C for 2 minutes, 42°C for 1 minute, 50°C for 1 second for 40 cycles, 85°C for 5 minutes then hold at 4°C. Obtained cDNA was diluted, mixed with TaqMan Gene Expression Master Mix, and loaded into each of the eight fill ports on the TaqMan® Human MicroRNA Array A (Life Technologies, Carlsbad, California, U.S.). The TaqMan Human MicroRNA Array is a 384-well microfluidics card containing 377 primer-probe sets for individual miRNAs as well as three carefully selected candidate endogenous small nucleolar RNAs control assay and one negative control assay. The array was centrifuged at 1.200 rpm twice for 1 minute each, then run on ABI-PRISM 7900 HT Sequence Detection System (Applied Biosystems). Two biological replicates were performed for each experimental condition. The data were quantified using the SDS 2.4 software and normalized using the RNU48 as endogenous control. The cycle threshold (Ct) value, which was calculated relatively to the endogenous control, was used for our analysis (ΔCt). The $2^{-\Delta\Delta CT}$ (delta-delta-Ct algorithm) method was used to calculate the relative changes in miRNA expression. A miRNA was defined differentially expressed when estimated P-value was $< 0.05$. As regards the differentially expressed miRNAs we established a cut off of fold change $> 1.5$ for up-regulated miRNAs and $< 0.5$ for down-regulated miRNAs.

## 3.5 Quantitative real-time PCR analysis

Quantitative real-time PCR was used to measure miRNA expression levels. Ten nanograms of total RNA were reverse transcribed using TaqMan MicroRNA Reverse Transcription Kit (Applied Biosystems, Foster City, CA, USA) according to manufacturer's instructions. RT reactions contained 10 ng of RNA sample, 100 nmol/l stem–loop RT primer, 100 mmol/l deoxynucleoside 5-triphosphates, 50 units/μl MultiscribeTM RT, 20 units/μl RNase inhibitor, 1·5 μl 10 × RT buffer (all from Applied Biosystems) and nuclease-free water. The 15-μl reactions were incubated in a Thermocycler (Eppendorf, North Ryde, New South Wales, Australia) for 30 min at 16°C, 30 min at 42°C, 5 min at 85°C and then held at 4°C.

The obtained cDNA was amplified using the following Taqman MicroRNA assays: hsa-miR-22, hsa-miR-24, hsa-miR-99a, hsa-miR-194, hsa-miR-214, hsa-miR-335, hsa-miR-339, hsa-miR-708 (Life Technologies, Carlsbad, CA, USA).

To normalize quantitative Real-Time PCR reactions, parallel reactions were run on each sample for RNU48 snRNA. The reactions were performed in triplicate and changes in the target miRNA content relative to RNU48 were determined using the comparative Ct method to calculate changes in Ct, and, ultimately, fold and percent change. An average Ct value for each RNA was obtained for replicate reactions.

## 3.6 miRNA Data Analysis

Hierarchical cluster and heat map analyses were performed using the MultiExperiment Viewer (MeV v4.8) program of TM4 Microarray Software Suite. Heat maps of miRNAs versus pathways were generated using miRPath v3.0 database, where the user can choose between in silico predicted miRNA gene targets and a large set of experimentally validated targets, or both (69). Information concerning MiRNA, mRNA target and related pathways was obtained from the literature and miRBase and Targetscan databases (111).

DIANA-miRPath v3.0 is based on a new relational schema, specifically designed to accommodate this as well as future miRPath updates. miRNA and pathway-related information was obtained from miRBase 18 (112) and Kyoto Encyclopedia of Genes and Genomes (KEGG) v58.1 (113).

Hierarchical clustering of targeted pathways and miRNAs was realized using DIANA-miRPath v3.0. The software created a clustering of the selected miRNAs based on their influence on molecular pathways (69).

## 3.7 Statistical analysis

The receiver operating characteristic (ROC) curves analysis were used to determine the optimal cut-off for each marker, in order to classify short-term versus long-term responders. The areas under the curves (AUC) were assessed to evaluate each marker performance for discriminating short from long-term survivors.

The analysis of PFS, defined as the time between blood sample collection and progression or death from any cause, was performed using the Kaplan-Meier method and log-rank test.

Univariate and multivariate Cox proportional hazard regression models were built in order to identify significant prognostic factors for PFS.

Data were generated using the MedCalc software for Windows, version 18.2.1 (MedCalc Software, Ostend, Belgium) and GraphPad Prism software v. 9.0.0 (GraphPad Software, San Diego, CA, USA). p-values $< 0.05$ were considered statistically significant.

One-way analysis of variance (ANOVA) test were used to perform analyses of correlation between pre-treatment (T0) ICs plasmatic levels in metastatic ccRCC patients of cohort number 2.

Fisher's exact test was used to evaluate the immunotherapy response based on the plasma PD-1, PD-L1, pan-BTN3As, BTN3A1, and BTN2A1 levels, respectively, and the correlation with the IMDC Prognostic Risk Group and number of metastatic sites. Wilcoxon test was used to evaluate paired samples. Pearson's chi-square test was used for association of sIC with best overall response by RECIST (BOR) and OR of >20%.

# 4. Results

## 4.1 Cohort Number 1

### 4.1.1 Clinico-Pathological Features of Metastatic GIST Patients

The study cohort includes 30 patients with a pathological diagnosis of advanced GIST, based on morphological characteristics and IHC for CD117 (KIT), carrying c-*KIT* exon 11 mutations who are candidates for first-line imatinib 400 mg/day in order to discover if soluble forms of immunomodulatory molecules, such as PD-1, PD-L1, BTN3A1, and pan-BTN3As, may be helpful in predicting the survival of metastatic GIST (mGIST) patients and to obtain significant information about the clinical evolution of disease..

We focused on c-*KIT* exon 11-mutated patients, because they represent the most common molecular subgroup in GISTs and, at the same time, show a wide variability in PFS to imatinib. Sixteen patients (53.3%) harbored c-*KIT* exon 11 deletion or delection/insertion, and 14 (46.7%) carried other PV types (duplication, insertion, or single nucleotide variant). The patients were mainly male (63%) and the median age at diagnosis was 58 years (mean 57; range 33–77 years). The most frequent site of primitive tumors was the stomach (14 patients; 46.7%), followed by the small bowel (11 patients; 36.6%) and, rarely, the GIST originated from other gastrointestinal sites (5 patients; 16.7%). The patients showed mainly larger primitive tumor (diameter > 5 cm) (18 patients; 60%) and higher mitotic index (mitoses > 5/50 HPF) (n = 17; 56.7%).

Regarding the metastatic site, 11 out of 30 patients (36.3%) had only hepatic metastases, 13 patients showed peritoneal metastases (43.4%), and 6 patients (20%) had both hepatic and peritoneal involvement. The clinical features and pathological parameters are shown in Table 2.

**Table 2. Clinico-pathological characteristics of metastatic GIST patients.**

| | | |
|---|---|---|
| Sex | Male | 19 (63.3) |
| | Female | 11 (36.7) |
| Age at Diagnosis | Median | 58 |
| | Mean | 57 |
| | Range | 33-77 |
| Age groups | ≤40 | 2 (6.6) |
| | 41-50 | 7 (23.4) |
| | 51-60 | 9 (30) |
| | >60 | 12 (40) |
| Type of *KIT* exon 11 PV | Deletion/Delins | 16 (53.3) |
| | Dupl/Inse/SNV | 14 (46.7) |
| Site of origin | Gastric | 14 (46.7) |
| | Small bowel | 11 (36.6) |
| | Other GI | 5 (16.7) |
| Primitive tumor diameter | ≤5 cm | 12 (40) |
| | >5 cm | 18 (60) |
| Mitosis | ≤5/50 HPF | 13 (43.3) |
| | >5/50 HPF | 17 (56.7) |
| Site of metastasis | Liver | 11 (36.6) |
| | Peritoneum | 13 (43.4) |
| | Liver and peritoneum | 6 (20) |
| PFS | ≤36 months | 20 (66.7) |
| | <36 months | 10 (33.3) |

### 4.1.2 Correlation between sICs and PFS

In order to establish for each soluble biomarker the optimal concentration threshold able to discriminate short-term survivors (STS) (≤36 months) versus long-term survivors (LTS) (>36 months) mGIST we performed the ROC curve. ROC curve analysis showed that the best cutoff concentration was 8.1 ng/mL for sPD-1 (AUC = 0.968, $p < 0.001$), 0.7 ng/mL for sPD-L1 (AUC = 1, 0, $p < 0.001$), 7.0 ng/mL for sBTN3A1 (AUC = 0.915, $p < 0.001$), and 5.0 ng/mL for pan-sBTN3As (AUC = 0.944, $p < 0.001$) (**Figure 3**)

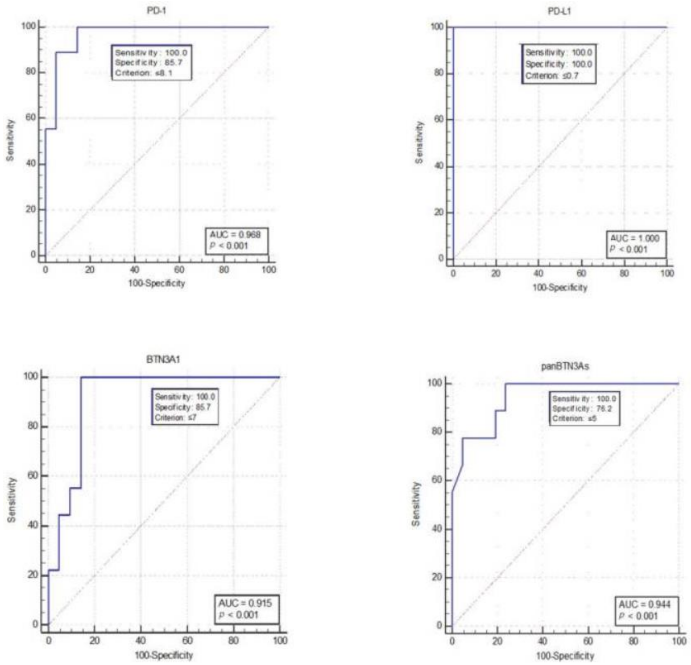


**Figure 3**: Analysis by ROC curves of circulating levels of sPD-1, sPD-L1, sBTN3A1, and pan-sBTN3As. The figure shows, for each circulating immune checkpoint, the best values of sensitivity and specificity to calculate the optimal concentration cut-offs (Youden index associated criterion). AUC, Area Under the Curve ROC. $p < 0.001$.

These values were found to be similar to the mean concentration values calculated for each soluble form of immune checkpoint tested, except for sBTN3A1. Indeed, the median concentration values were 8.91 ng/mL for sPD-1 (range 2.29 to 24.22 ng/mL), 1.06 ng/mL for sPD-L1 (range 0.30 to 2.22 ng/mL), 9.07 ng/mL for sBTN3A1 (range 0.70 to 13.53 ng/mL), and 5.66 ng/mL for pan-sBTN3A (range 0 to 9.36 ng /mL).

Most patients with LTS mGIST showed lower plasma levels for each soluble biomarker (sPD-1, sPD-L1, sBTN3A1 and pan-sBTN3As), than patients with STS, highlighting the high predictive power of all soluble forms. (**Figure 4**)

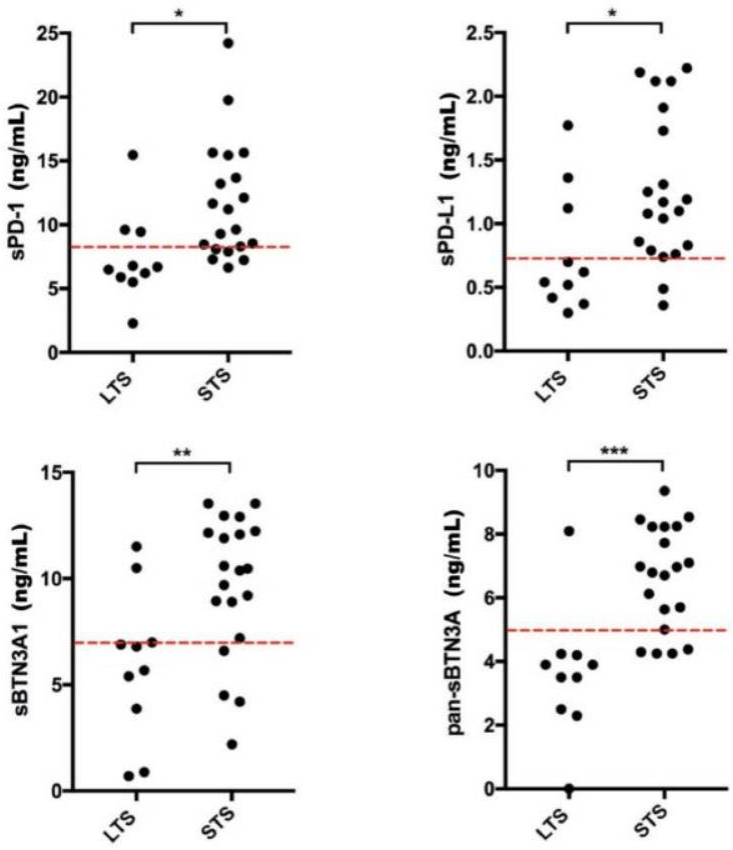


**Figure 4**: Scatter plot by group discriminating STS and LTS mGIST patients. The plasma concentrations of each soluble protein were graphically represented for short-term survival (STS) and long-term survival (LTS) patients. For each circulating immune checkpoint, the red dotted lines point out the best concentration threshold previously determined through ROC analysis. The concentrations are shown in ng/mL. * $p < 0.05$; ** $p = 0.007$; *** $p = 0.0001$.

In order to understand the potential prognostic value of plasma PD-1, PD-L1, BTN3A1 and pan-BTN3A in patients with advanced GIST, we classified mGIST patients based on the plasma concentrations for each tested biomarker obtained by ROC analysis and subsequently we calculated PFS using Kaplan-Meier curves (**Figure 5**)

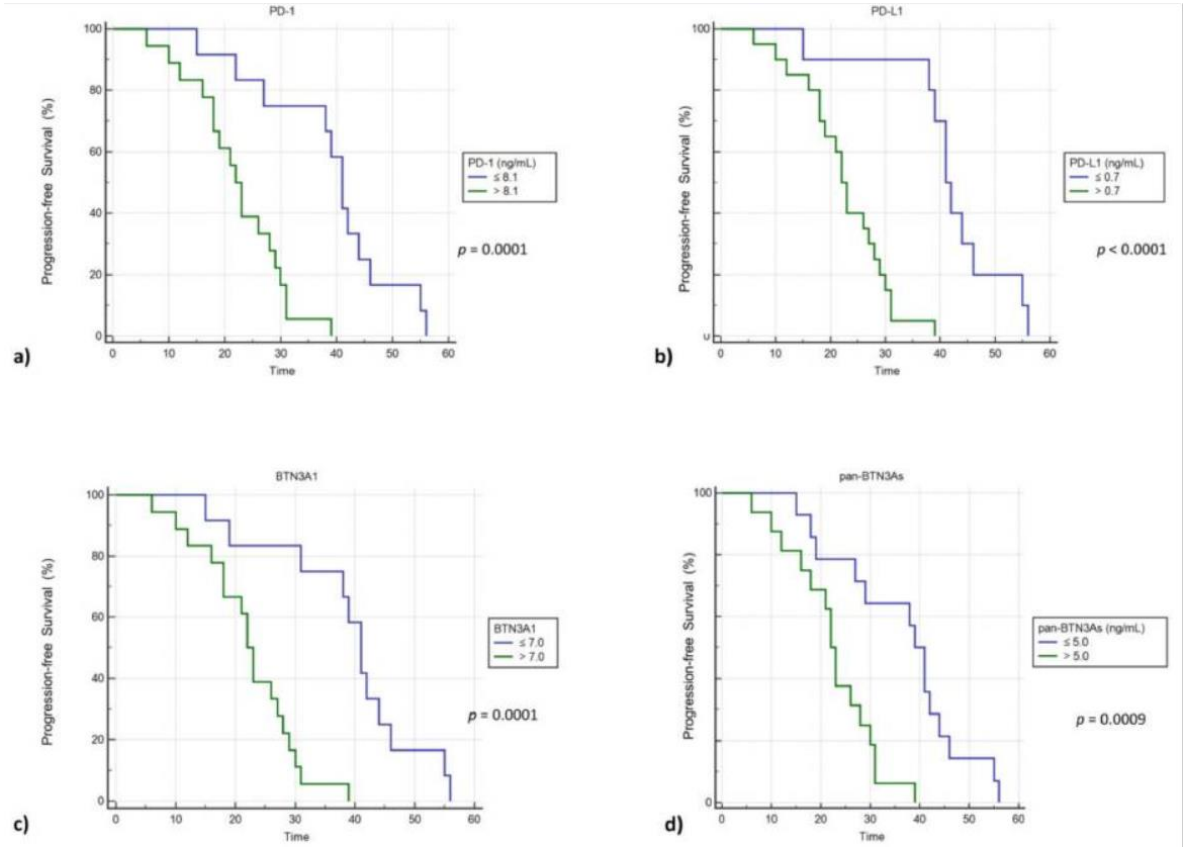


**Figure 5**: PFS analysis by Kaplan–Meier curves in 30 mGIST patients with baseline high and low plasma concentrations of sPD-1 (a), sPD-L1 (b), sBTN3A1 (c), and pan-sBTN3As (d).

For each tested protein, patients with plasma concentrations above and under thresholds showed statistically significant differences in PFS. Particularly, plasma concentration cut-offs associated with unfavorable prognosis and shorter survival were determined for sPD-1 (>8.1 ng/mL), sPD-L1 (>0.7 ng/mL), sBTN3A1 (>7.0 ng/mL), and pan-sBTN3As (>5.0 ng/mL) while individuals with plasma concentrations below the thresholds had a median PFS that was approximately 20 months longer. Specifically, patients with an elevated baseline level of sPD-1 (>8.1 ng/mL), sPD-L1 (>0.7 ng/mL), and sBTN3A1 (>7.0 ng/mL) showed a Median PFS of 22 months versus 41 months for subjects who had lower levels of sPD-1 (log-rank p value = 0.0001, value < 0.0001) and sBTN3A1 (log-rank p value = 0, 0001). The same association was observed for pan-sBTN3A (22 months vs. 39 months; log-rank p-value = 0.0009) (Figure 4). Thus, the soluble forms of all ICs studied in this work have been shown to be potential survival factors in patients with mGIST.

### 4.1.3 Multivariate Analysis of Prognostic Factors for PFS

We performed a multivariate analysis for PFS in order to correlate the type of KIT exon 11 mutation detected in our population cohort, plasma immune checkpoint levels, and other clinical factors, based on literature data demonstrating the correlation between type of mutations and response to imatinib. In particular, the presence of deletions at codons 557/558 was found to be linked to significantly shorter PFS than point mutations (PMID: 33673554).

The results of this multivariate analysis are reported in Table 3.

Univariate analysis showed that plasma sPD-1, sPD-L1, sBTN3A1 and pan-sBTN3A levels, age at diagnosis, and KIT exon 11 PV type were statistically significantly associated with PFS , whereas in the final multivariable Cox regression model only plasma sPD-L1 levels ≤ 0.7 ng/mL (HR: 0.01; 95% CI: 0.001 to 0.18; p = 0.001), pan- sBTN3As ≤ 5.0 ng/mL (HR: 4.45; 95% CI: 0.96 to 20.5; p = 0.05) and the absence of KIT exon 11 Del or Delins at codons 557 and/or 558 (HR: 0.05; 95% CI: 0.007 to 0.31; p = 0.003) were statistically significant.

**Table 3:** Univariate and multivariate analysis of prognostic factors for PFS in KIT exon 11-mutated mGIST patients treated with first-line imatinib.

| PFS | Univariate Cox Regression | | Multivariable Cox Regression | |
|---|---|---|---|---|
| | HR (95% CI) | *p*-Value | HR (95% CI) | *p*-Value |
| Gender (M vs. F) | 0.90 (0.42–1.98) | NS | - | - |
| Age (≤55 vs. >55 years) | 2.25 (1.01–4.98) | 0.04 | 0.93 (0.33–2.61) | NS |
| Primitive tumor diameter (≤5 cm vs. >5 cm) | 0.67 (0.31–1.47) | NS | - | - |
| Mitosis (≤5/50 HPF vs. >5/50 HPF) | 0.74 (0.34–1.62) | NS | - | - |
| Gastric site of origin (No vs. yes) | 0.68 (0.31–1.45) | NS | - | - |
| sPD-L1 (≤0.7 vs. >0.7 ng/mL) | 0.05 (0.01–0.25) | <0.0001 | 0.01 (0.001–0.18) | 0.001 |
| sPD-1 (≤8.1 vs. >8.1 ng/mL) | 0.16 (0.05–0.45) | 0.0001 | 1.85 (0.47–7.27) | NS |
| sBTN3 A1 (≤0.7 vs. >0.7 ng/mL) | 0.14 (0.05–0.41) | 0.0001 | 0.84 (0.17–4.23) | NS |
| pan-sBTN3 s (≤5.0 vs. >5.0 ng/mL) | 0.23 (0.09–0.58) | <0.001 | 4.45 (0.96–20.5) | 0.05 |
| *KIT* exon 11 Del or Delins at codons 557 and/or 558 (No vs. yes) | 0.04 (0.008–0.35) | <0.001 | 0.05 (0.007–0.31) | 0.003 |

Therefore, our analysis highlighted that the absence of KIT exon 11 deletions or delins at codons 557 and/or 558 and expression levels of sPD-L1 ≤ 0.7 ng/mL and pan-sBTN3As ≤ 5.0 ng/mL were independent prognostic factors associated with a longer PFS in mGIST patients harboring a KIT exon 11 PV prior to imatinib therapy (**Figure 6**).

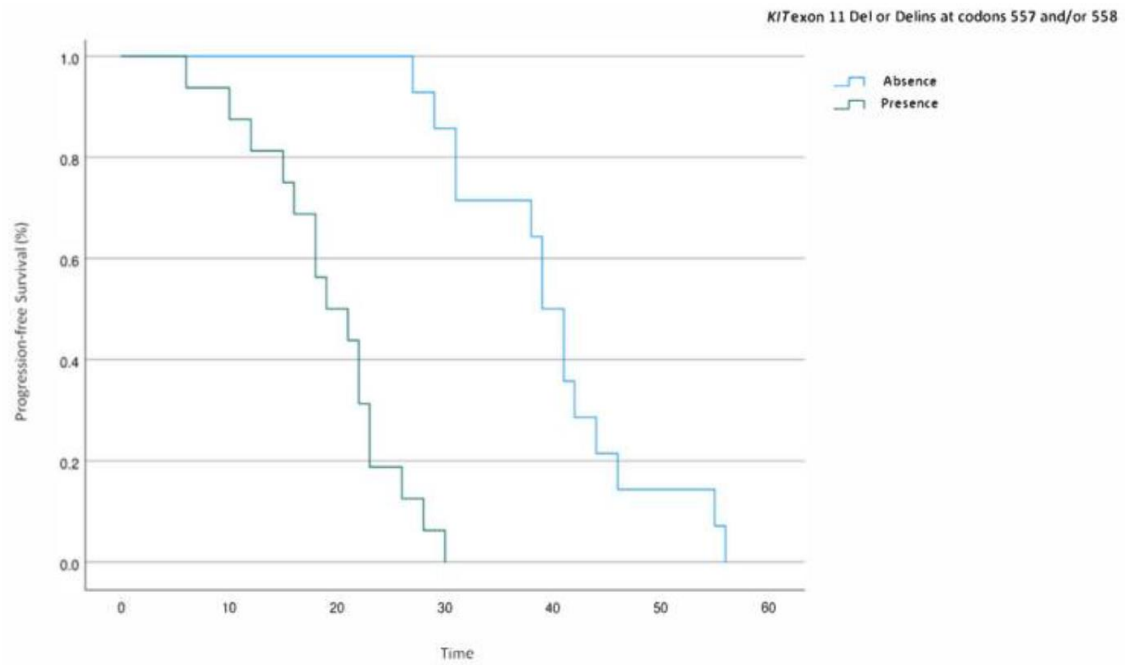


**Figure 6**: PFS analysis in mGIST patients harboring KIT exon 11 deletions or delins at codons 557 and/or 558.

## 4.2 Cohort Number 2

### 4.2.1 Clinico-Pathological Features of metastatic clear cell renal cell carcinoma (mccRCC) patients

The study included fifty-six (56) patients with ccRCC. Of these, twenty-one (21) were metastatic patients from the learning cohort treated with second-line nivolumab, twenty (20) were patients from an independent validation cohort of mccRCC patients receiving nivolumab to confirm levels of correlation among each sIC tested, fifteen (15) were ccRCC patients with localized disease included in the exploratory analysis. The clinicopathological characteristics of the population are summarized in Table 4.

We investigated the potential role of sPD-1, sPD-L1, and sBTNs (pan-sBTN3A, sBTN3A1, and sBTN2A1) levels as predictive biomarkers of response to nivolumab treatment in mccRCC patients

**Table 4:** Clinical and pathological features of metastatic and localized RCC patients

| Baseline characteristics Tot (n) | 21 |
|---|---|
| Median age (range) – years | 61 (36–70) |
| Sex, n (%) | |
| Male | 19 (90.5%) |
| Female | 2 (9.5%) |
| Histological classification | |
| Clear cell | 21 (100%) |
| Other | 0 (0%) |
| Prior nephrectomy | |
| Yes | 5 (23.8%) |
| No | 16 (76.2%) |
| No. of evaluable disease sites, n (%) | |
| ≤2 | 4 (19.1%) |
| ≥3 | 17 (80.9%) |
| Site of metastasis | |
| Lung only | 6 (28.6%) |
| Lung + others | 15 (71.4) |
| Site of metastasis, individual | |
| Lung | 10 (47.6%) |
| Lymph node | 11 (52.4%) |
| Liver | 6 (28.6%) |
| Bone | 5 (23.8%) |
| Pancreas | 1 (4.7%) |
| SNC | 4 (19%) |
| IMDC Prognostic Risk Group, n (%) | |
| Favorable | 6 (28.6%) |
| Intermediate | 15 (71.4%) |
| Poor | 0 (0%) |
| Best response to nivolumab treatment | |
| Complete response (CR) | 1 (4.7%) |
| Partial response (PR) | 9 (42.9%) |
| Stable disease (SD) | 10 (47.7%) |
| Progressive disease (PD) | 1 (4.7%) |
| Median duration of response (range) – months | 14 (3–28) |

| Baseline characteristics Tot (n) | 15 |
|---|---|
| Median age (range) – years | 61 (31–87) |
| Sex | |
| Male | 11 (73.3%) |
| Female | 4 (26.7%) |
| Histological classification | |
| Clear cell | 15 (100%) |
| Others | 0 (0%) |
| Type of surgery | |
| Partial Nephrectomy | 7 (46.7%) |
| Radical Nephrectomy | 8 (53.3%) |
| AJCC/UICC TNM classification | |
| Stage I | 7 (46.7%) |
| Stage II | 5 (33.3%) |
| Stage III | 3 (20%) |

### 4.2.2 Baseline plasma ICs levels as predictive biomarkers of anti-PD-1 treatment outcome in mRCC patients

Plasma sPD1 and sPD-L1 levels were analyzed in blood samples from 21 mRCC patients from the learning cohort before nivolumab treatment (T0). The mean sPD1 and sPD-L1 levels were 2.79 ng/ml (range 0.52-25.00) and 0.62 ng/ml (range 0.26-1.31), respectively.

The same analysis was performed on soluble butyrophylline-like receptors, such as sBTN3global, sBTN3A1 and sBTN2A1. Mean plasma levels were 12.65 ng/ml (range 3.32–28.18), 7.00 ng/ml (range 2.03–24.76), and 8.66 ng/ml (range 5,67–16,93), respectively.

To investigate the predictive role of plasma ICs levels in response to immunotherapy, sICs levels prior to nivolumab treatment (T0) were correlated with PFS and best overall response by RECIST.

Based on the PFS compared to nivolumab treatment we divided the patients into 3 groups:

- 2 patients showed a PFS <6 months;
- 10 patients showed a PFS between 6 and 18 months;
- 9 patients showed a PFS>18 months.

Comparing the mean pre-treatment (T0) levels of plasma ICs of all patients with the long-responder group (>18 months), sPD1, sPD-L1, and sBTN3A1 were higher in long-responder patients: 13.25 ng/ml (range 1.22–25.0), 1.09 ng/ml (range 0.47–2.41), and 11.03 (9.32–24.76) for sPD-1, sPD-L1, and sBTN3A1, respectively. These difference were statistically significant (p = 0.01; p = 0.02; p = 0.03) (**Figure 7**).

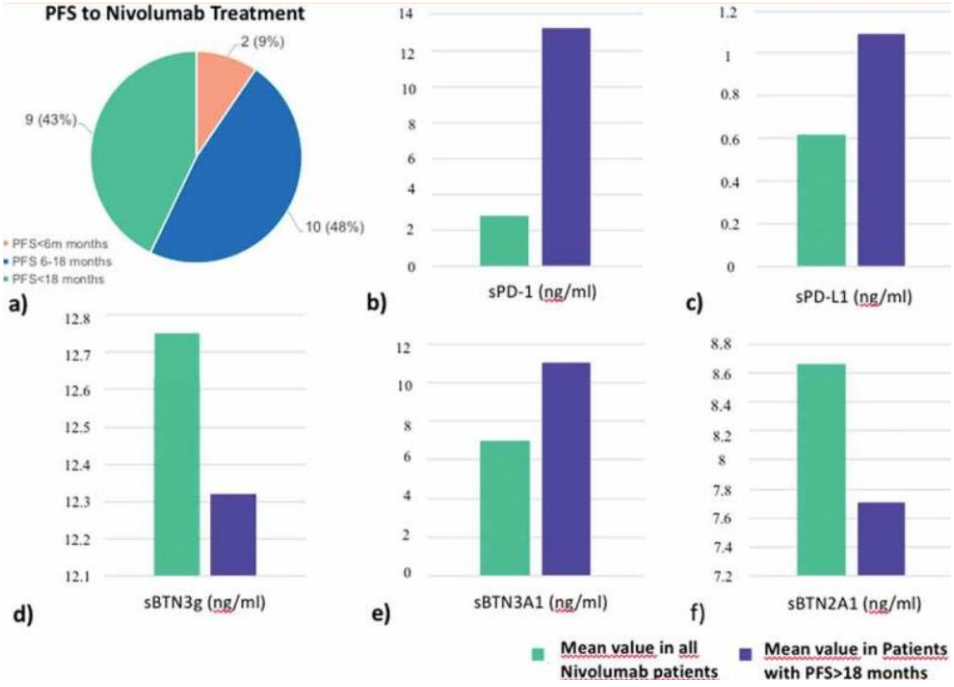


**Figure 7**: PFS (months) to nivolumab treatment in mccRCC patients (a); mean value of plasmatic ICs levels in all nivolumab patients versus long-responders patients (>18 months) (b, c–f).

For butyrophyllines, The mean plasma levels of sBTN3 global and sBTN2A1 in patients with PFS>18 months were 12.32 ng/ml (range 7.79–27.77) and 7.71 (range 4.91–10.00) ng/ml, respectively (Figure 2(d,f)), but the difference for these three ICs, if compared with all nivolumab patients, was not statistically significant. For this reason, they were not included in the further survival analyses.

Using specific cut-offs determined from the ROC curves, we divided patients based on low and high plasma levels for each ICs analyzed and calculated PFS using Kaplan-Meier curves. (**Figure 8**)

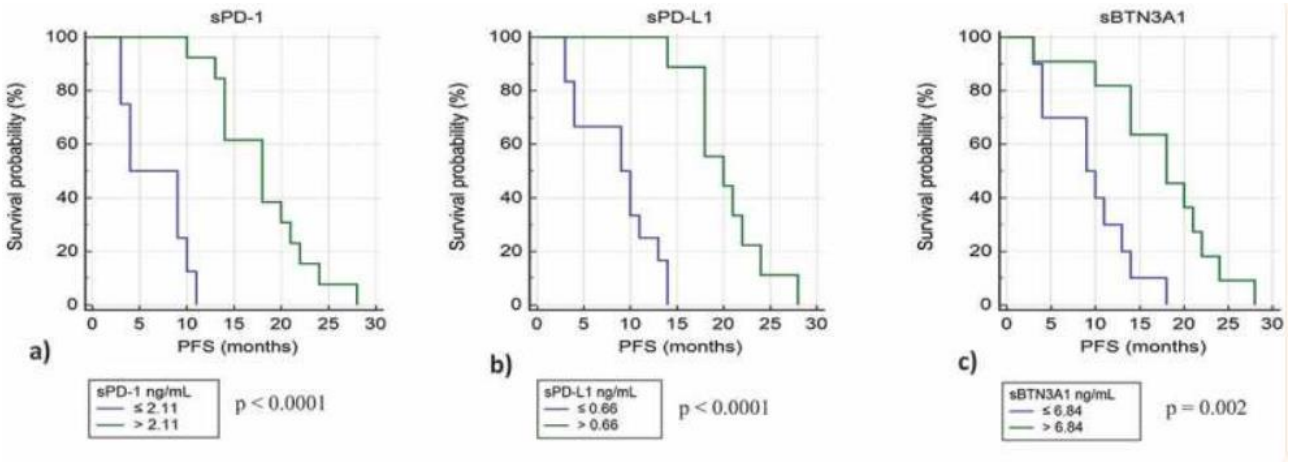


**Figure 8**: Kaplan-Meier analysis of progression free survival in patients from learning cohort with high and low plasma levels of sPD-1 (a), sPD-L1 (b), and sBTN3A1 (c)

For sPD-1, sPD-L1, and sBTN3A1 we observed strong significant differences in median PFS between patients with plasma concentrations above and under thresholds. Patients with high levels of sPD-1 (>2.11 ng/ml) have a median PFS of 20.7 months compared to 6.9 months for patients with low levels of sPD-1 (p value < 0.0001). Patients with high levels of sPD-L1 (>0.66 ng/ml) have a median PFS of 19 months compared to 9 months for patients with low levels of sPD-L1 (p value < 0.0001), and patients with high levels of sBTN3A1 (>6.84 ng/ml) have a median PFS of 17.5 months compared to 8.4 months for patients with low levels of BTN3A1 (p value = 0.002). The strongest difference in PFS was observed using sPD-1 as biomarker.

The association of sIC with best overall response by RECIST (BOR) and objective response of >20% (OR) were also analyzed. High sPD-1 (>2.11 ng/ml) and sBTN3A1 (>6.84 ng/ml) levels were associated with BOR, but also with favorable OR (objective response of >20%).

We investigated the correlation between baseline plasma levels of ICs and some clinical factors, including the location of distant metastases (lung vs other sites), the number of metastatic sites (≤2 or ≥3) and the IMDC prognostic risk group. Regarding the location of distant metastases and the number of metastatic sites, the levels of sPD-L1 and sBTN2A1 were increased in patients with non-pulmonary metastases compared with lung-only (sPD-L1 p = 0.003; sBTN2A1 p = 0.01) and were significantly higher in patients with ≥3 sites of disease (sPD-L1 p = 0.03; sBTN2A1 p = 0.003).

The association between higher sPD-L1 levels and the IMDC intermediate risk group was also found (p = 0.003).

### 4.2.3 Comparison T0-T1 of ICs levels in the plasma of mccRCC long responders patients treated with nivolumab

In *long responders* patients (PFS>18 months), after a 4-weeks period (T1) with nivolumab treatment (2 cycles of nivolumab administration), plasma levels of sPD1 and sPD-L1 were lower than baseline, with a mean of 1.23 ng/ml (range 1.06–1.93) for sPD-1 and 0.73 ng/ml (range 0.56–1.39) for sPD-L1 while plasma levels of sBTN2A1 were higher at the 4-weeks period (T1; 9.99 ng/ml; range 7.94–19.13) than baseline (T0; mean 7.71 ng/ml; range 4.91–10.0).

Wilcoxon test for paired samples showed a statistically significant difference between T0 and T1 for both sPD1 and sBTN2A1 (sPD1: T0 vs T1 p = .0078; sBTN2A1 T0 vs T1 p = 0.0007), probably the small number of analyzed samples did not allow us to demonstrate a statistically significant difference in T0-T1 sPD-L1 levels (p = 0.097). The paired-sample Wilcoxon test showed a statistically significant difference between T0 and T1 for both sPD1 and sBTN2A1 (sPD1: T0 vs T1 p = 0.0078; sBTN2A1 T0 vs T1 p = 0.0007), although perhaps the small number of analyzed samples did not allow to demonstrate a statistically significant difference in T0-T1 sPD-L1 levels (p = 0.097). Changes in plasma levels are showed also for sBTN3A1 and sBTN3 global, but these difference T0-T1 did not reach statistical significance.

### 4.2.4 Exploratory analysis: comparison of plasma ICs levels in metastatic versus localized ccRCC patients

Plasma levels of ICs were analyzed in 15 patients with localized RCC before surgery and were compared with the metastatic cohort. The concentrations of sPD-1, sPD-L1, sBTN2A1 e sBTN3A1 were statistically higher in the plasma of metastatic patients than in patients with localized RCC. Mean sPD-1 in localized group was 1.54 ng/ml (range 0.55–3.91) vs mean sPD-1 in metastatic group 2.79 ng/ml (range 0.52–25.00). Mean sPD-L1 in localized group was 0.49 ng/ml (range 0.25–0.69) vs mean sPD-L1 in metastatic group 0.62 ng/ml (range 0.26–2.41) (sPD-1 p = 0.003; sPD-L1 p = 0.03).

Mean values of sBTN2A1 e sBTN3A1 were higher in the group of metastatic compared to the group of localized patients, but the difference between the two groups is not statistically significant (BTN2A1: 8.33 vs 8.66 ng/ml; BTN3A1: 6.47 vs 7.01 ng/ml). (**Figure 9**)

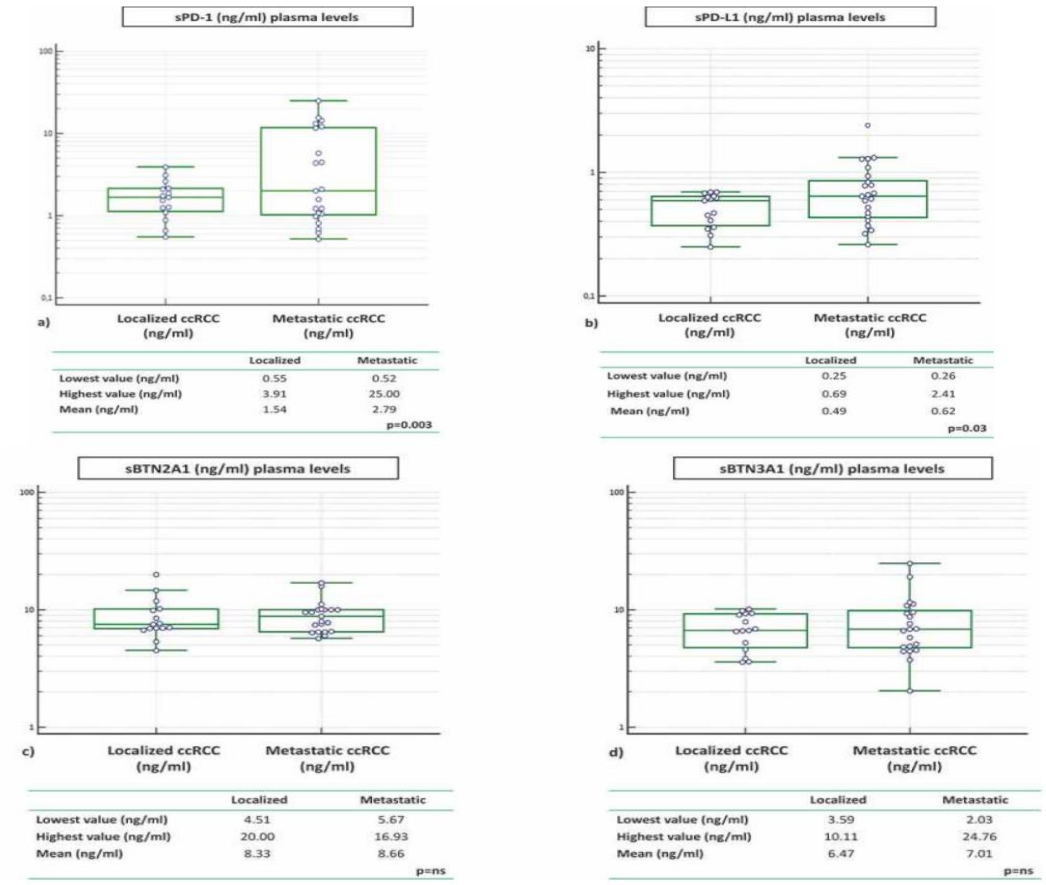


**Figure 9**: ICs in RCC patients: localized vs metastatic disease at baseline (pretreatment)

### 4.2.5 Analysis in the validation cohort

To confirm the predictive value of the tested ICs, we used 20 independent blood samples from mccRCC patients. In this cohort, the optimal cut-off was 1.31 ng/ml (AUC = 1.0, p value < 0.001) for sPD-1, 0.73 ng/ml for sPD-L1 (AUC = 0.944, p value < 0.001), 3.8 ng/ml for sBTN3A1 (AUC = 0.806, p value < 0.03), 5.11 ng/ml for sBTN3 global (AUC = 0.833, p value < 0.01), and 9.12 ng/ml for sBTN2A1 (AUC = 0.708, p value 0.23).

Subsequently, applying to the validation cohort the threshold levels previously determined in the learning cohort from the ROC curves, we found a significant correlation between PFS and anti-PD-1 treatment and high baseline expression levels in plasma for sPD-1, sPD- L1 and sBTN3A1. These data confirmed our previous results in the learning cohort and allowed to discriminate *short* versus *long-responders* to nivolumab therapy in the validation cohort. Patients with high levels of sPD-1 (>2.11 ng/ml) had a median PFS of 16.6 months compared to 9.7 months for patients with low levels of sPD-1 (p value = 0.002); patients with high levels of sPD-L1 (>0.66 ng/ml) had a median PFS of 15.7 months compared to 8.6 months for patients with low levels of sPD-L1 (p value < 0.003).

Concerning patients with high levels of sBTN3A1 (>6.84 ng/ml), they had a median PFS of 16.9 months compared to 7.8 months for patients with low levels of BTN3A1 (p value < 0.001).

## 4.3 Cohort Number 3

### 4.3.1 Clinico-Pathological Features of metastatic clear cell renal cell carcinoma (mccRCC) patients

The study included twenty-three metastatic ccRCC patients treated with second-line nivolumab in order to investigate the association between the plasma levels of sPD-1/sPD-L1 and expression of lymphocyte miRNAs. The clinical and pathological characteristics of the study population are summarized in the Table 5.

**Table 5**: Clinical and pathological features of metastatic renal cell carcinoma (mRCC) patients.

| Baseline Characteristics | |
|---|---|
| **Tot (No.)** | **23** |
| Median Age (range)—years | 62 (36–71) |
| Sex, *n.* (%) | |
| Male | 19 (82.6%) |
| Female | 4 (17.4%) |
| Histological classification | |
| Clear cell | 23 (100%) |
| Other | 0 (0%) |
| Prior nephrectomy | |
| Yes | 7 (30.4%) |
| No | 16 (69.6%) |
| No. of evaluable disease sites, *n* (%) | |
| ≤2 | 5 (19.1%) |
| Site of metastasis | |
| Lung only | 7 (30.4%) |
| Lung + others | 16 (69.6) |
| Site of metastasis, individual | |
| Lung | 11 (47.8%) |
| Lymph node | 12 (52.2%) |
| Liver | 6 (26.1%) |
| Bone | 5 (21.7%) |
| Pancreas | 1 (4.3%) |
| SNC | 4 (17.4%) |
| IMDC Prognostic Risk Group, *n* (%) | |
| Favorable | 6 (26.1%) |
| Intermediate | 17 (73.9%) |
| Poor | 0 (0%) |
| Best response to nivolumab treatment | |
| Complete Response (CR) | 1 (4.3%) |
| Partial Response (PR) | 9 (39.2%) |
| Stable Disease (SD) | 11 (47.8%) |
| Progressive Disease (PD) | 2 (8.7%) |
| Median duration of response (range) -months | 15 (3–29) |

### 4.3.2 Expression Profile of Lymphocyte miRNAs as Predictive Biomarkers of Anti-PD-1 Treatment Outcome

In order to study the effect of nivolumab treatment on the miRNA expression profile in lymphocytes we performed a large-scale analysis of 377 miRNAs on peripheral blood samples before nivolumab treatment (T0) and after a 4-week period (T1) with nivolumab treatment (2 cycles of nivolumab administration).

Among all 377 analyzed miRNAs, microarray analysis showed 66 differentially expressed miRNAs in peripheral lymphocytes between T0 and T1. Sixty-four miRNAs were upregulated, and only 2 miRNAs were downregulated at T1 versus T0.

To investigate the predictive role of lymphocyte miRNA expression profile in response to immunotherapy, we divided patients into 3 groups based on PFS to nivolumab treatment and best overall response by RECIST (complete response, CR; partial response, PR ; stable disease response, SD; disease progression, PD):

- group A: 2/23 patients with PFS <6 months;
- group B: 11/23 patients with PFS between 6-18 months;
- group C: 9/23 patients with PFS>18 months.

We compared the lymphocyte miRNA expression profile between three groups and in order to highlight significantly expressed miRNAs, we established a fold change (FC) cutoff >2 for upregulated miRNAs and FC<0.3 for downregulated miRNAs ( $p < 0.05$).

After 4 weeks of nivolumab treatment (T1), patients with SD, PR, or CR as best responders showed 28 lymphocyte miRNAs specifically induced by nivolumab treatment, which were silenced at T0, of which 21 were related to the of clear cell renal cancer signaling (analysis conducted using the DIANA-mirPath v.3.0 tool). (**Table 6**)

**Table 6** : microRNAs induced by Nivolumab treatment

| **microRNAs** | | | |
|---|---|---|---|
| miR-99a | miR-708 | miR-655 | miR-582-3p |
| miR-492 | miR-487a | miR-485-3p | miR-449a |
| miR-433 | miR-431 | miR-429 | miR-376c |
| miR-342-5p | miR-340 | miR-339-5p | miR-335 |
| miR-324-5p | miR-25 | miR-24 | miR-22 |
| miR-221 | miR-214 | miR-194 | miR-18b |
| miR-152 | miR-143 | miR-100 | miR-let-7e |

Subsequently, a statistical analysis, performed by assessing only the intersection of targeted genes (hypothetical genes targeted by all selected miRNAs), revealed the involvement of 26 out of the 28 miRNAs and 183 miRNA-targeted genes involved in the PI3K-Akt signaling pathway, one of the most significant pathways in cancer biology (Table 7).

**Table 7**: Cellular pathways modulated by 28 specific miRNAs induced by Nivolumab.

| Pathway | miRNAs | No. of Gene Targets |
|---|---|---|
| PI3K-Akt signaling | 26 | 183 |
| MAPK signaling | 24 | 130 |
| T-cell receptor signaling | 24 | 55 |
| Hippo signaling | 22 | 87 |
| FOXO signaling | 22 | 75 |
| HIF-1 signaling | 22 | 56 |
| mTOR signaling | 20 | 35 |

Other miRNA-related molecular pathways were MAPK signaling (130 genes, 24 miRNAs), T-cell receptor (55 genes, 24 miRNAs), Hippo signaling (87 genes, 22 miRNAs), FOXO signaling (75 genes, 22 miRNAs). 22 miRNAs) miRNA), HIF-1 signaling pathway (56 genes, 22 miRNA), mTOR signaling (35 genes, 20 miRNA) (Table 3). Our analysis showed that miRNAs are potential molecular mediators through which nivolumab can exert its antitumor activity.

In order to investigate the predictive role of deregulated lymphocyte miRNAs, we evaluated the expression of some specific miRNAs induced exclusively after nivolumab treatment in long-responder patients. A subset of 8 specific miRNAs strongly induced by nivolumab treatment was identified in this subset of patients. These 8 miRNAs, which included miR-22, miR-24, miR-99a, miR-194, miR-214, miR-335, miR-339, miR-708, were found only in peripheral lymphocytes of long-responder patients (>18 months) and were found to be specifically and highly induced by nivolumab treatment (**Table 8**)

**Table 8**: microRNAs induced by nivolumab treatment.

| miRNAs | Mean Ct Value | Gene Targets |
|---|---|---|
| **miR-22** | 12.86 | AKT3 |
| **miR-24** | 7.80 | MAPK1 |
| **miR-99a** | 17.63 | GSK3B, GIMAP1, TMEM71, TIAM1, PDE4D, TRABD2A, SCGN, CUX1, CD93, EIF1, HIPK1, FNTA, LRRC28 |
| **miR-194** | 16.74 | STAT6, PCDHA4, IRF1, NOS1 |
| **miR-214** | 16.81 | PIK3CB, PAK3, PAK6 |
| **miR-335** | 17.82 | MET, SOS2, PIK3CB, PAK2/3, TGF-A, AKT3, ETS1, PIK3R1, PIK3CG, PIK3CA, CREBBP, EGLN1 |
| **miR-339** | 15.77 | PIK3CB, SOS1, PAK6, VEGFA |
| **miR-708** | 17.81 | SOS2, CRK, CDC42 |

These results were confirmed through quantitative real-time PCR analysis in an independent validation cohort of 8 mccRCC patients.

An enrichment analysis carried out using online tools available from The Database for Annotation, Visualization and Integrated Discovery (DAVID) allowed us to identify 41 KEGG pathways modulated by the "lymphocyte signature" of 8 miRNAs, including several signaling pathways related to renal cell carcinoma.

### 4.3.3 Association Between Lymphocyte miRNA Expression and Plasma Levels of Soluble PD-1/PD-L1 in Long-Responders Patients

In 9 patients long-responders to treatment with nivolumab we studied the association between plasma sPD-1/sPD-L1 levels and lymphocyte miRNA expression profile, in order to investigate the translational potential of miRNAs in regulating ICs expression. In this patient cohort, we showed that miR-22 and miR-24 levels were inversely correlated with plasma PD-1 levels. At baseline (T0), high sPD-1 levels were observed (median 13.15 ng/mL; range: 1.12–25.00), whereas the expression of lymphocyte miR-22/miR-24 was silenced (Ct > 40). Conversely, after 4 weeks from starting nivolumab (T1), sPD-1 levels were strongly reduced (median 1.25 ng/mL; range: 1.06–1.97) and the expression of miR-22/miR-24 was restored (mean Ct: 12.86 and 7.80, respectively) only in patients with PR/CR/SD to nivolumab >18 months (p = 0.007), suggesting that a miRNA network could inhibit sPD-1 expression mainly via miR-20 family. In the same way, an inverse correlation between sPD-L1 and lymphocyte miR-22 and miR-24 was showed (T0, median value: 1.1 ng/mL; range 0.46–2.41; T1, median value: 0.71 ng/mL; range 0.55–1.39), but, probably, the small number of analyzed samples did not allow us to demonstrate a statistically significant difference between T0 and T1 (p = 0.09). (**Figure 10**)

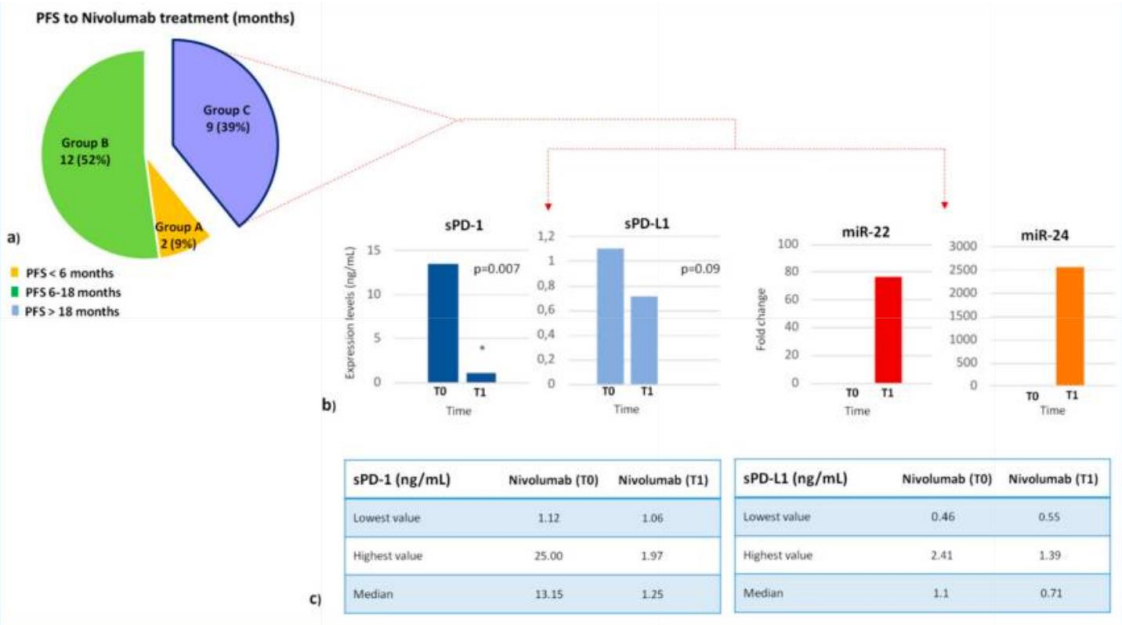


c)

| sPD-1 (ng/mL) | Nivolumab (T0) | Nivolumab (T1) |
|---|---|---|
| Lowest value | 1.12 | 1.06 |
| Highest value | 25.00 | 1.97 |
| Median | 13.15 | 1.25 |

| sPD-L1 (ng/mL) | Nivolumab (T0) | Nivolumab (T1) |
|---|---|---|
| Lowest value | 0.46 | 0.55 |
| Highest value | 2.41 | 1.39 |
| Median | 1.1 | 0.71 |

**Figure 10**: Correlation between expression of miRNAs 22/24 and plasma levels of soluble PD-1/PD-L1 in a group of 9 long-responder patients.

## 4.4 Cohort Number 4

### 4.4.1 Clinico-Pathological Features of metastatic melanoma patients

This study included a cohort of 41 patients with a histologically confirmed diagnosis of melanoma, harboring no BRAF, NRAS, or KIT mutations, candidates for first-line treatment based on anti-PD-1 nivolumab or pembrolizumab.

The purpose of the study was to investigate the role of BMI and baseline plasma levels of sPD-1, sPD-L1, sBTN2A1 and sBTN3A1 as predictive biomarkers of immunotherapy response in metastatic melanoma patients treated with anti-PD-1 nivolumab or pembrolizumab as first-line treatment.

Clinical features of metastatic melanoma patients are summarized in Table 9.

**Table 9 :** Clinical features of metastatic melanoma patients.

| Characteristic | No. of patients (%) |
|---|---|
| No. of patients | 41 |
| Gender | |
| Male | 23 (56) |
| Female | 18 (44) |
| Age at diagnosis (year) | |
| Median | 49 |
| Mean | 50.6 |
| Range | 23–74 |
| Age groups (years) | |
| ⩽40 | 10 (24.4) |
| 41–50 | 13 (31.7) |
| 51–60 | 6 (14.6) |
| >60 | 12 (29.3) |
| Type of melanoma | |
| Cutaneous | 29 (70.7) |
| Uveal | 5 (12.2) |
| Mucosal | 2 (4.9) |
| Unknown origin | 5 (12.2) |
| Primary cutaneous tumor site | |
| Limbs (acral) | 11 (38) |
| Head and neck | 7 (24.1) |
| Back | 7 (24.1) |
| Chest | 2 (6.9) |
| Abdomen | 2 (6.9) |
| TILs | |
| Brisk | 10 (24.4) |
| Non-brisk | 6 (14.6) |
| Absent | 12 (29.3) |
| NA | 13 (31.7) |
| Site of metastasis, individual | |
| Lymph nodes | 31 (75.6) |
| Lung | 19 (46.3) |
| Liver | 16 (39) |
| Skin | 14 (34.1 |
| Bones | 9 (22) |
| CNS | 8 (19.5) |
| Soft tissues | 8 (19.5) |
| Adrenal gland | 6 (14.6) |
| Others | 18 (43.9) |
| LDH* | |
| ⩽300 | 21 (51.2) |
| >300 | 20 (48.8) |
| NLR* | |
| ⩽2.6 | 23 (56.1) |
| >2.6 | 18 (43.9) |
| BMI* | |
| BMI < 25 | 16 (39) |
| BMI ⩾ 25 | 25 (61) |
| Best response to nivolumab/pembrolizumab | |
| CR and PR | 16 (39) |
| SD | 12 (29) |
| PD | 13 (32) |

### 4.4.2 Outcome analysis

In order to evaluate the role of the soluble form of sPD-1, sPD-L1, sBTN3A1 and sBTN2A1 as predictive markers of response to immunotherapy, we classified the plasma levels of each biomarker tested as "low" or "high" concentrations based on the thresholds calculated through the ROC analysis. The primary clinical outcome of the study was TTF, defined as the time from immunotherapy initiation to discontinuation for any reason excluding remission, i.e. disease progression, treatment toxicity, patient preference, or death.

Overall median TTF was 36 months [95% confidence interval (CI): 14.3–57.7]. At the time of data analyses, a total of 26 events (progression or death) occurred (63.4%). Notably, the presence of plasma levels of sPD-1 < 11.24 ng/ml and sBTN2A1 ⩾ 4.0 ng/ml was significantly associated with longer TTF (Figure 2(h) and ((l)).l)). Regarding the outcome data according to plasma levels of sPD-1, 7 events were observed in the group of 20 patients with sPD-1 low levels (35%), and 19 events in the group of 21 patients with sPD-1 high levels (90.4%). Regarding the outcome data according to plasma levels of sBTN2A1, 16 events were observed in the group of 20 patients with sBTN2A1 low levels (80%), and 10 events in the group of 21 patients with sBTN2A1 high levels (47.6%). Median TTF was not reached (NR) for the low sPD-1 group, and 17 months (95% CI: 5.0, 28.9) for the high sPD-1 group ($p < 0.002$).

In contrast, pre-treatment PD-1 levels were higher in patients who did not respond to immunotherapy treatment, whereas pre-treatment levels of circulating BTN2A1 were significantly lower in patients who did not respond to treatment. No significant differences were observed for circulating PD-L1 and BTN3A1.

The next goal was the calculation of the OS. Overall median OS was 107 months (95% CI: 88.7, 125.3). In all, 23 total events (deaths) were observed (56.1%). The distribution of events according to sPD-1 concentrations was: 10 in 20 patients with low sPD-1 levels (50%) and 13 in 21 patients with high sPD-1 levels (61.9%). Median OS was 108 months (95% CI: 21.1, 194.8) and 88 months (95% CI: 45.6, 130.3) for the low and high sPD-1 groups, respectively ($p = 0.03$) (Figure 3(h)). The difference was not significant for the other sICs (**Figure 11**)

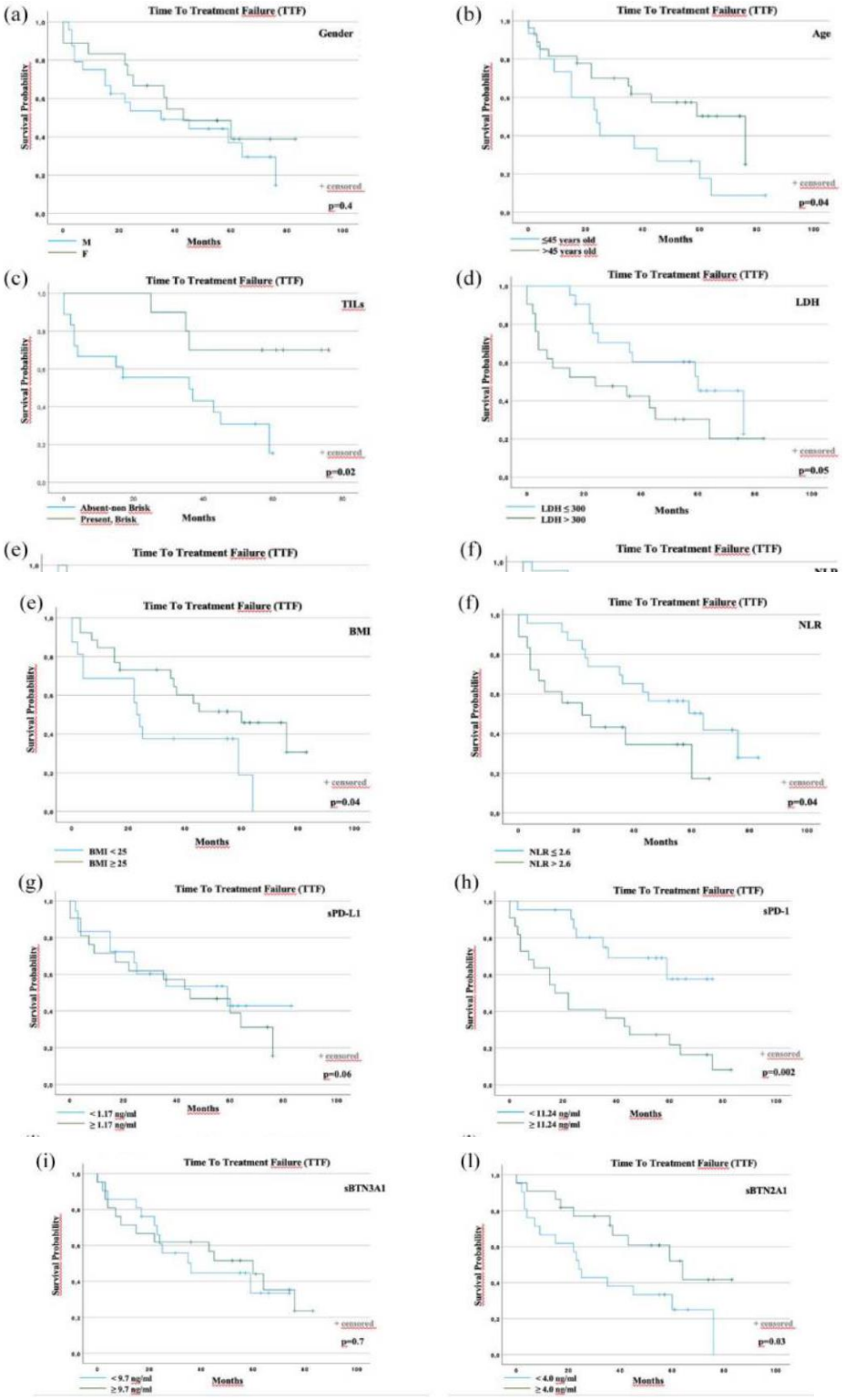


**Figure 11**: TTF according to prognostic factors.

### 4.4.3 ORR

We evaluated the association between ORR and pretreatment levels of sPD-1 and sBTN2A1, which were previously significant in survival analyses.

After first-line anti-PD-1 treatment, patients showed the following best response: 16 PR/CR patients (39%), 12 SD patients (29%) and 13 PD patients (32%).

Patients with low sPD-1 levels before treatment had a significantly higher ORR (ORR 65%; n = 13/20 patients) than patients with high sPD-1 levels (ORR: 14.3%, 3/ 21 patients) (p =0.001) (Figure 4(b)), while patients with high sBTN2A1 levels at baseline had a significantly higher ORR (ORR 60%; n = 12/20 patients) than patients with low levels of sBTN2A1 (ORR 19%, 4/21 patients) (p = 0.01).

Next, we assessed the level of sPD-L1 and sBTN2A1 in "long" and "short" responder patients using the previously calculated median TTF to anti-PD-1 therapy. In long-responders patients we observed significantly lower sPD-1 levels (10.3 ng/ml, range: 1.7–16.1) and significantly higher sBTN2A1 levels (4.4 ng/ml, range: 3.0–9.4) (p = 0.001 and p = 0.004, respectively) compared with short-responders (sPD-1: 16.6 ng/ml, range: 8.3–25.0; sBTN2A: 3.77 ng/ml, range: 1.7–5.7).

Therefore, higher levels of sPD-1 and lower levels of sBTN2A1 before the treatment were associated with poorer clinical outcomes and ORR (**Figure 12**)

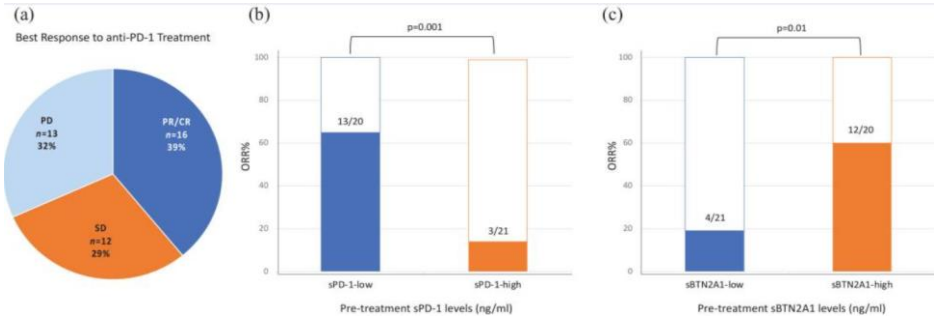


**Figure 12**: ORR in the groups of patients showing high and low sPD-1 and sBTN2A1 pretreatment plasma levels.

ORR, objective response rate; sBTN, soluble butyrophilin; sPD-1, soluble programmed cell death protein 1.

### 4.4.4 Multivariable analysis

Variables included in the univariate analysis were as follows: (1) gender (male or female); (2) age at first-line start (⩽45 or >45 years); (3) TILs in primary melanoma (absent/non-brisk or present brisk); (4) BMI at first-line start (<25 or ⩾25); (5) NLR at first-line start (⩽2.6 or >2.6); (6) serum pretreatment level of LDH (⩽300 or >300); (7) baseline plasma levels of sPD-L1 (<1.17 or ⩾1.17 ng/ml); (8) baseline plasma levels of sPD-1 (<11.24 or ⩾11.24 ng/ml); (9) baseline plasma levels of sBTN3A1 (<9.7 or ⩾9.7 ng/ml); and (10) baseline plasma levels of sBTN2A1 (<4.0 or ⩾4.0 ng/ml).

Univariate analyzes showed that age, BMI, NLR, sPD-1 and sBTN2A1 are statistically significantly associated with TTF, whereas in the final multivariable Cox regression model, only BMI [p = 0.02, hazard ratio (HR): 0.37] and sPD-1 (p = 0.002, HR: 4 ,5) were significant.

Regarding OS, LDH and sPD-1 were statistically significantly associated with univariate analyses. In the final multivariable model, no prognostic factor considered remains statistically significant.

These results demonstrate that in metastatic melanoma patients treated with first-line PD-1 inhibitors, BMI ⩾ 25 and sPD-1 < 11.24 ng/ml were significant independent prognostic factors for longer TTF.

The association between BMI and ORR showed that BMI ⩾ 25 is related to higher response rates compared to patients of normal weight [48% (12 of 25) vs. 25% (4 of 16)] (p = 0.001). Specifically, patients with a BMI of 25 or higher and sPD-1 < 11.24 ng/ml had improved TTF (median TTF NR) following ICI treatment than patients with a BMI of less than 25 and sPD-1 ⩾ 11.24 ng/ml (median TTF 4 months, 95% CI, 2.8–5.2). (**Figure 13**)

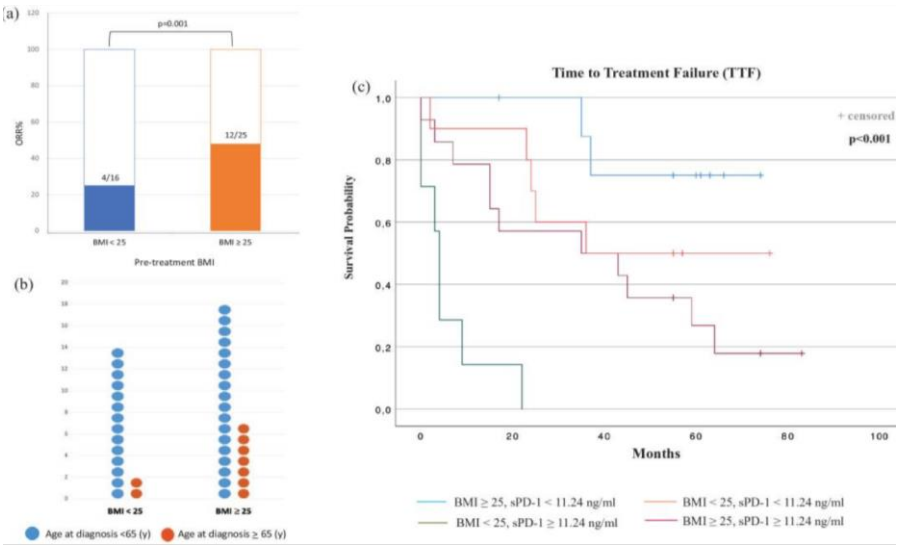


**Figure 13**: ORRs according to the BMI (a), BMI and age at diagnosis (b), and TTF analyses of melanoma patients stratified by BMI and sPD-1 (c).

BMI, body mass index; ORRs, objective response rates; sPD-1, soluble programmed cell death protein 1; TTF, time to treatment failure.

Results on the potential role of exosomes in mccRCC and melanoma patients undergoing immunotherapy treatment and their correlation with PD-1/PD-L1 are still ongoing. However, the preliminary data obtained appear in line with literature data which highlight their potential role as important players in the immunomodulatory response mediated by PD-1/PD-L1.

The first analyzes carried out show a correlation between high levels of PD-L1 and a shorter PFS in both cohorts of patients analyzed. Therefore, further investigations will be needed to obtain more accurate results

# 5. Discussion

In recent years, inhibition of the PD-1/PD-L1 immune regulatory complex through the development of targeted monoclonal antibodies has resulted in interesting results in phase II and III clinical trials for the clinical management of various solid tumours with consequent improvements in the prognosis of patients with advanced disease (114, 115).

This evidence showed that effective blockade of PD-1 attachment to PD-L1 can activate the antitumour immune response and increase patient survival in a variety of cancers, making immunotherapy a clinically validated and effective therapeutic option for some cancers such as NSCLC, melanoma and RCC (116).

Despite significant clinical benefit and durable responses, the percentage of patients who can benefit is rather low due to resistance mechanisms (117, 118). Therefore, identifying precise and dynamic biomarkers capable of guiding the selective treatment of patients who could benefit from immunotherapy is a need that is not yet completely fulfilled.

Until now, the only predictive biomarker used as a companion diagnostic test for first-line immunotherapy is PD-L1 expression assessed by IHC from tissue sections, although it has several technical and biological limitations, as well as heterogeneous intra- and inter-tumour expression (92). In several cancer types, high tumour expression of PD-L1 in tissue is associated with a poor prognosis (119, 120). PD-L1 expression in tumours is strongly correlated with a poor prognosis in gastric carcinoma, hepatocellular carcinoma, RCC, esophageal cancer, pancreatic cancer and ovarian carcinoma (121-123).

Opposite results were observed in breast carcinoma and Merkel cell carcinoma, where tumour PD-L1 expression correlates with a better prognosis (124).

Since PD-L1 and PD-1 are dynamic molecules and their tissue expression in the tumour cannot provide an overview of the tumour disease and its evolution, the study of soluble forms of ICs, detected in plasma or serum, could be a valuable prognostic factor in several types of solid tumours (109, 124, 125).

To this end, our study assessed plasma concentrations of sPD-1, sPD-L1, sBTN3A1 and pan-sBTN3A in mGISTs and their relationship with PFS showed a negative correlation, demonstrating for the first time that the assessment of plasma concentrations of certain ICs could help predict survival in advanced GIST patients. Plasma levels of sPD-L1 $\leq$ 0.7 ng/mL and pan-sBTN3As $\leq$ 5.0 ng/mL, and the absence of KIT exon 11 deletions or delins at codons 557 and/or 558 were significant prognostic factors for a longer PFS in mGIST patients.

In RCC the role of sICs has not been well investigated. An early study by Frigola et al. (doi: 10.1158/1078-0432.ccr-10-0250) showed for the first time that an elevated preoperative serum level of sPD-L1 was associated with an increased risk of death in patients with ccRCC. Several studies, including KEYNOTE-427 and CheckMate 214, observed an increased PFS and response rate in PD-L1+ tumours (doi: 10.1200/jco.2014.59.0703; doi: 10.1016/s1470-2045(19)30413-9). Also in our study, we observed that baseline levels of sPD-1, sPD-L1 and sBTN3A1 were associated with longer PFS, best overall response according to RECIST and >20% objective response, demonstrating the role of sPD-1, sPD-L1 and sBTN3A1 in predicting response to therapy.

The treatment paradigm for mRCC continues to evolve with new insights into the molecular biology and immunological background of renal tumours (126). In particular, epigenetic modifications, such as aberrant DNA methylation or abnormal expression of miRNAs, are emerging as central features of renal tumours (127).

Based on this evidence, we hypothesised that an expression profile of miRNAs directly identified in peripheral lymphocytes of patients before and after immunotherapy administration could be useful to assess the dynamic molecular changes underlying nivolumab therapy and predict treatment response. Our study revealed several differentially expressed miRNAs in peripheral lymphocytes of long-responder patients, most of which are implicated in major RCC signalling pathways involving VHL-HIF, PI3K/Akt, MAPK cascade, mTOR, FOXO and receptor T cells. In particular, we found a specific subset of miRNAs (miR-22, miR-24, miR-99a, miR-194, miR-214, miR-335, miR-339, miR-708), which we termed "lymphocyte miRNA signature", specifically and exclusively induced in long-responders recognised as patients with CR, PR or SD to nivolumab > 18 months. This mechanism of miRNA restoration in responder patients could be useful to identify potential biomarkers predictive of therapy efficacy and response to nivolumab.

Among the miRNAs specifically induced by nivolumab, miR-22, also in other studies has been found to be downregulated in both serum and tissues of ccRCC patients and thus could act as a tumour suppressor, as its loss of expression could contribute to the development of RCC through PTEN-mediated induction of cell proliferation, migration and invasion (128). These data suggest that the miR-22/PTEN axis could be considered new potential therapeutic targets useful for the development of effective therapeutic strategies against RCC (129).

Opposite results were instead reported by Gong et *al*. (130) showing a correlation between miR-22 and cell proliferation and invasion in primary in vitro cultures of ccRCC.

Contrasting data were also reported for miR-24, which in our analysis showed high and specific induction after immunotherapy treatment (131, 132).

A potential tumour-suppressive role mediated by the mTOR pathway has been attributed to miR-99a, as it has been observed that this miRNA is downregulated in RCC tissues, correlating with poor survival in RCC patients, and that its overexpression induces G-phase cell cycle arrest, inhibiting cell growth and tumorigenicity (133), supporting our results. However, a more recent study by Oliveira et *al*. (134) showed increased expression of miR-99a and downregulation of its target gene mTOR in ccRCC tissue samples, hypothesising a potential oncogenic role for this miRNA.

In support of our findings, other literature data show miR-194 as a favourable prognostic biomarker implicated in the inhibition of tumour progression and therapy resistance in RCC (135, 136).

Furthermore, miR-214 has been shown to inhibit RCC cell proliferation through downregulation of insulin-like growth factor-1 (IGF-1) receptor expression levels and inhibition of downstream mTORC1 signalling, independent of VHL status (137). In contrast, low expression levels of miR-214 were associated with increased cell growth and reduced drug sensitivity in RCC cells (138).

It was also observed that upregulation of miR-335 suppresses the proliferation and invasion of ccRCC cells through direct repression of the BCL-W gene, whereas its downregulation is significantly associated with the occurrence of lymph node metastases and increased tumour size (139).

Further evidence supporting our results is the potential association between downregulation of miR-339 and increased tumour PD-L1 expression, resulting in attenuation of the antitumour immune response in RCC patients. Therefore, the induction of miR-339 expression after nivolumab treatment is congruent with the longer PFS observed in our cohort of long response patients. Finally, miR-708 has been shown to induce apoptosis and inhibit cell growth, invasion, migration and tumorigenicity in renal cancer cells and in murine xenograft models of human RCC (140).

Furthermore, we evaluated the correlation between the signature of lymphocyte miRNAs identified in RCC long-responders and plasma levels of sPD-1/sPD-L1 in order to assess the clinical translational potential of miRNAs in modulating immune checkpoint expression (141).

Previous studies have shown that miR-200 expression negatively correlates with PD-L1 expression (142), that baseline levels of sPD-1 and sPD-L1 were associated with longer PFS treatment, and that high levels of sPD-1 was also associated with better overall response according to RECIST and objective response of >20% (143, 144). In our study, the inverse correlation between miR-22 and miR-24 levels and plasma PD-1 levels in long-responder patients suggests that a miRNA network might inhibit immune checkpoint expression, mainly through the miR-20 family.

In our cohort of patients with metastatic melanoma stratified by BMI, we observed that patients with metastatic melanoma with BMI>25 and low plasma PD-1 levels (sPD-1 <11.24 ng/ml) assessed at baseline, had nivolumab or pembrolizumab first-line with TTF and ORR. One possible reason why low plasma sPD-1 is more strongly associated with TTF is that sPD-1 might represent a direct target

of anti-PD-1 immunotherapy and therefore a high plasma concentration of sPD-1 may compromise the efficacy of ICIs by neutralising the PD-1 inhibitors pembrolizumab and nivolumab, resulting in treatment resistance and shorter TTF (145).

Although this hypothesis is interesting, it does not explain the better clinical results obtained in overweight melanoma patients showing low sPD-1 levels, which could instead be explained by PD-1-mediated T-cell dysfunction induced by excess adiposity (146).

Obesity promotes a systemic and chronic inflammatory state (145), which can induce immunosuppression as a result of a protective mechanism against possible autoreactive responses of the immune system (PMID: 35241833), alters the adipose tissue microenvironment, stimulates the production of pro-inflammatory cytokines and elevated levels of insulin, glucose, fatty acids and leptin (147, 148).

A recent study suggests the role of leptin signalling in increasing PD-1 expression and promoting T-cell depletion, resulting in an immunosuppressed phenotype and obesity-related T-cell ageing (146). Therefore, our data showing lower sPD-1 concentrations in overweight patients responding to anti-PD-1 antibodies could be indicative of a lower state of CD8+ T-cell depletion and dysfunction.

# 6. Conclusions

Recent studies have shown that the PD-1/PD-L1 axis is responsible for less than half of the dysfunctional anti-tumor immunity in cancers, suggesting that other mechanisms are involved in tumor immune evasion.

Butyrophilins and butyrophilin-like family of proteins, such as BTN2A1, BTN3A1, and BTNL2, have been shown to play a critical role in modulating γδ T cell development and differentiation. Recent clinical studies reported the modified expression of molecules belonging to the BTN/BTNL family and PD1/PD-L1 axis following immune checkpoint blockade with anti-PD-1 antibodies, suggesting their unexplored role in tumor immune evasion.

Furthermore, the new and evolving role of patients' metabolic state and systemic inflammation is now highlighted, in complex symbiotic and metabolic interactions between tumor cell and dysfunctional/suppressive immune cells in the TME. Since several clinical data showed that obesity is paradoxically associated with improved outcomes in cancer patients treated with immune checkpoint blockade, tumor metabolic dependencies are emerging as key tumor vulnerabilities, and patient-associated features, such as body mass index, are under investigation as factors to profoundly impact the cancer immune responses. Although the mechanistic link between metabolic state and immunotherapy benefit was not elucidated, an impact of excess adiposity/obesity on the PD-1/PD-L1 pathway seems to exist.

Our study on the role of plasma levels of soluble PD-1, PD-L1, BTN2A1 and BTN3A1, as prognostic and/or predictive biomarkers of treatment response in metastatic melanoma, renal cancer and GIST patients, suggest that circulating ICs detection, could be an useful tool to predict the response to specific treatment, discriminating responders from non-responders already at therapy baseline, with the advantages of non-invasive sample collection and real-time monitoring that allow to assess the dynamic changes during cancer evolution and treatment. Future studies in a larger patient cohort should be encouraged to validate these preliminary results.

## Article

1. L. Incorvaia, D. Fanale, G. Badalamenti, **C. Brando**, M. Bono, I. De Luca, L. Algeri, A. Bonasera, L.R. Corsini, S. Scurria, J.L. Iovanna, A. Russo and V. Bazan. ***A "lymphocyte microRNA signature" as predictive biomarker of immunotherapy response and plasma PD-1/PD-L1 expression levels in patients with metastatic renal cell carcinoma: pointing towards epigenetic reprogramming.*** Oncoimmunology, 2020; 12(11):E3396. doi: 10.3390/cancers12113396.

2. L. Incorvaia, D. Fanale, G. Badalamenti, C. Porta, D. Olive, I. De Luca, **C. Brando**, M. Rizzo, C. Messina, M. Rediti, A. Russo, Viviana Bazan & Juan Lucio Iovanna. ***Baseline plasma levels of soluble PD-1, PD-L1, and BTN3A1 predict response to nivolumab treatment in patients with metastatic renal cell carcinoma: a step toward a biomarker for therapeutic decisions.*** Oncoimmunology, 2020; 9(1):1832348. doi: 10.1080/2162402X.2020.1832348

3. D. Fanale, L. Incorvaia, G. Badalamenti, I. De Luca, L. Algeri, A. Bonasera, L.R. Corsini, **C. Brando**, A. Russo, J.L. Iovanna, V. Bazan. ***Prognostic Role of Plasma PD-1, PD-L1, pan-BTN3As and BTN3A1 in Patients Affected by Metastatic Gastrointestinal Stromal Tumors: Can Immune Checkpoints Act as a Sentinel for Short-Term Survival?*** Cancers, 2021; 13(9): 2118. doi: 10.3390/cancers13092118.

4. Incorvaia L, Rinaldi G, Badalamenti G, Cucinella A, **Brando C**, Madonia G, Fiorino A, Pipitone A, Perez A, Li Pomi F, Galvano A, Gristina V, Barraco N, Bono M, Bazan Russo TD, Toia F, Cordova A, Fanale D, Russo A, Bazan V. ***Prognostic role of soluble PD-1 and BTN2A1 in overweight melanoma patients treated with nivolumab or pembrolizumab: finding the missing links in the symbiotic immune-metabolic interplay.*** Ther Adv Med Oncol. 2023 Feb 15;15:17588359231151845. doi: 10.1177/17588359231151845. PMID: 36818688; PMCID: PMC9936535.

## Other article related

1. D. Fanale*, L.R. Corsini*, **C. Brando***, S. Cutaia, M.C. Di Donna, C. Filorizzo, M.C. Lisanti, U. Randazzo, L. Magrin, R. Romano, T.D. Bazan Russo, D. Olive, S. Vieni, G. Pantuso, V. Chiantera, A. Russo, V. Bazan, J.L. Iovanna. ***Can circulating PD-1, PD-L1, BTN3A1, pan-BTN3As, BTN2A1 and BTLA levels enhance prognostic power of CA125 in patients with advanced high-grade serous ovarian cancer?*** Front. Oncol., 2022; 12: 946319. doi: 10.3389/fonc.2022.946319.

   * These authors contributed equally to this work.

2. Fanale D*, **Brando C***, Corsini LR*, Cutaia S, Di Donna MC, Randazzo U, Filorizzo C, Lisanti C, Magrin L, Gurrera V, Romano R, Dimino A, Bazan Russo TD, Olive D, Vieni S, Pantuso G, Giordano A, Chiantera V, Russo A, Bazan V, Iovanna JL. ***Low plasma PD-L1 levels, early tumor onset and absence of peritoneal carcinomatosis improve prognosis of women with advanced high-grade serous ovarian cancer.*** BMC Cancer. 2023 May 13;23(1):437. doi: 10.1186/s12885-023-10911-5. PMID: 37179293; PMCID: PMC10183131.

   * These authors contributed equally to this work.

## References


1. Gonzalez H, Hagerling C, Werb Z. Roles of the immune system in cancer: from tumor initiation to metastatic progression. Genes Dev. 2018;32(19-20):1267-84.
2. Smyth MJ, Dunn GP, Schreiber RD. Cancer immunosurveillance and immunoediting: the roles of immunity in suppressing tumor development and shaping tumor immunogenicity. Adv Immunol. 2006;90:1-50.
3. Muenst S, Läubli H, Soysal SD, Zippelius A, Tzankov A, Hoeller S. The immune system and cancer evasion strategies: therapeutic concepts. J Intern Med. 2016;279(6):541-62.
4. Abbott M, Ustoyev Y. Cancer and the Immune System: The History and Background of Immunotherapy. Semin Oncol Nurs. 2019;35(5):150923.
5. Ghosh C, Luong G, Sun Y. A snapshot of the PD-1/PD-L1 pathway. J Cancer. 2021;12(9):2735-46.
6. Yi M, Jiao D, Xu H, Liu Q, Zhao W, Han X, et al. Biomarkers for predicting efficacy of PD-1/PD-L1 inhibitors. Mol Cancer. 2018;17(1):129.
7. Marei HE, Hasan A, Pozzoli G, Cenciarelli C. Cancer immunotherapy with immune checkpoint inhibitors (ICIs): potential, mechanisms of resistance, and strategies for reinvigorating T cell responsiveness when resistance is acquired. Cancer Cell Int. 2023;23(1):64.
8. Zhu X, Lang J. Soluble PD-1 and PD-L1: predictive and prognostic significance in cancer. Oncotarget. 2017;8(57):97671-82.
9. Han Y, Liu D, Li L. PD-1/PD-L1 pathway: current researches in cancer. Am J Cancer Res. 2020;10(3):727-42.
10. Yi M, Niu M, Xu L, Luo S, Wu K. Regulation of PD-L1 expression in the tumor microenvironment. J Hematol Oncol. 2021;14(1):10.
11. Akbay EA, Koyama S, Carretero J, Altabef A, Tchaicha JH, Christensen CL, et al. Activation of the PD-1 pathway contributes to immune escape in EGFR-driven lung tumors. Cancer Discov. 2013;3(12):1355-63.
12. Ota K, Azuma K, Kawahara A, Hattori S, Iwama E, Tanizaki J, et al. Induction of PD-L1 Expression by the EML4-ALK Oncoprotein and Downstream Signaling Pathways in Non-Small Cell Lung Cancer. Clin Cancer Res. 2015;21(17):4014-21.
13. Fang W, Zhang J, Hong S, Zhan J, Chen N, Qin T, et al. EBV-driven LMP1 and IFN-γ up-regulate PD-L1 in nasopharyngeal carcinoma: Implications for oncotargeted therapy. Oncotarget. 2014;5(23):12189-202.
14. Xu L, Chen X, Shen M, Yang DR, Fang L, Weng G, et al. Inhibition of IL-6-JAK/Stat3 signaling in castration-resistant prostate cancer cells enhances the NK cell-mediated cytotoxicity via alteration of PD-L1/NKG2D ligand levels. Mol Oncol. 2018;12(3):269-86.
15. Niu M, Liu Y, Yi M, Jiao D, Wu K. Biological Characteristics and Clinical Significance of Soluble PD-1/PD-L1 and Exosomal PD-L1 in Cancer. Front Immunol. 2022;13:827921.
16. Merelli B, Massi D, Cattaneo L, Mandalà M. Targeting the PD1/PD-L1 axis in melanoma: biological rationale, clinical challenges and opportunities. Crit Rev Oncol Hematol. 2014;89(1):140-65.
17. Zhang Y, Zhang Z. The history and advances in cancer immunotherapy: understanding the characteristics of tumor-infiltrating immune cells and their therapeutic implications. Cell Mol Immunol. 2020;17(8):807-21.
18. Korman AJ, Garrett-Thomson SC, Lonberg N. The foundations of immune checkpoint blockade and the ipilimumab approval decennial. Nat Rev Drug Discov. 2022;21(7):509-28.
19. Shiravand Y, Khodadadi F, Kashani SMA, Hosseini-Fard SR, Hosseini S, Sadeghirad H, et al. Immune Checkpoint Inhibitors in Cancer Therapy. Curr Oncol. 2022;29(5):3044-60.
20. Tang Q, Chen Y, Li X, Long S, Shi Y, Yu Y, et al. The role of PD-1/PD-L1 and application of immune-checkpoint inhibitors in human cancers. Front Immunol. 2022;13:964442.
21. Alley EW, Lopez J, Santoro A, Morosky A, Saraf S, Piperdi B, et al. Clinical safety and activity of pembrolizumab in patients with malignant pleural mesothelioma (KEYNOTE-028): preliminary results from a non-randomised, open-label, phase 1b trial. Lancet Oncol. 2017;18(5):623-30.
22. Hodi FS, Chiarion-Sileni V, Gonzalez R, Grob JJ, Rutkowski P, Cowey CL, et al. Nivolumab plus ipilimumab or nivolumab alone versus ipilimumab alone in advanced melanoma (CheckMate 067): 4-year outcomes of a multicentre, randomised, phase 3 trial. Lancet Oncol. 2018;19(11):1480-92.
23. Stratigos AJ, Garbe C, Dessinioti C, Lebbe C, Bataille V, Bastholt L, et al. European interdisciplinary guideline on invasive squamous cell carcinoma of the skin: Part 2. Treatment. Eur J Cancer. 2020;128:83-102.

24. Knight A, Karapetyan L, Kirkwood JM. Immunotherapy in Melanoma: Recent Advances and Future Directions. Cancers (Basel). 2023;15(4).
25. Larkin J, Chiarion-Sileni V, Gonzalez R, Grob JJ, Cowey CL, Lao CD, et al. Combined Nivolumab and Ipilimumab or Monotherapy in Untreated Melanoma. N Engl J Med. 2015;373(1):23-34.
26. Postow MA, Chesney J, Pavlick AC, Robert C, Grossmann K, McDermott D, et al. Nivolumab and ipilimumab versus ipilimumab in untreated melanoma. N Engl J Med. 2015;372(21):2006-17.
27. Gandhi L, Rodríguez-Abreu D, Gadgeel S, Esteban E, Felip E, De Angelis F, et al. Pembrolizumab plus Chemotherapy in Metastatic Non-Small-Cell Lung Cancer. N Engl J Med. 2018;378(22):2078-92.
28. Rittmeyer A, Barlesi F, Waterkamp D, Park K, Ciardiello F, von Pawel J, et al. Atezolizumab versus docetaxel in patients with previously treated non-small-cell lung cancer (OAK): a phase 3, open-label, multicentre randomised controlled trial. Lancet. 2017;389(10066):255-65.
29. Ravi P, Mantia C, Su C, Sorenson K, Elhag D, Rathi N, et al. Evaluation of the Safety and Efficacy of Immunotherapy Rechallenge in Patients With Renal Cell Carcinoma. JAMA Oncol. 2020;6(10):1606-10.
30. Horn L, Mansfield AS, Szczęsna A, Havel L, Krzakowski M, Hochmair MJ, et al. First-Line Atezolizumab plus Chemotherapy in Extensive-Stage Small-Cell Lung Cancer. N Engl J Med. 2018;379(23):2220-9.
31. Schmid P, Adams S, Rugo HS, Schneeweiss A, Barrios CH, Iwata H, et al. Atezolizumab and Nab-Paclitaxel in Advanced Triple-Negative Breast Cancer. N Engl J Med. 2018;379(22):2108-21.
32. Chung HC, Ros W, Delord JP, Perets R, Italiano A, Shapira-Frommer R, et al. Efficacy and Safety of Pembrolizumab in Previously Treated Advanced Cervical Cancer: Results From the Phase II KEYNOTE-158 Study. J Clin Oncol. 2019;37(17):1470-8.
33. Powles T, Durán I, van der Heijden MS, Loriot Y, Vogelzang NJ, De Giorgi U, et al. Atezolizumab versus chemotherapy in patients with platinum-treated locally advanced or metastatic urothelial carcinoma (IMvigor211): a multicentre, open-label, phase 3 randomised controlled trial. Lancet. 2018;391(10122):748-57.
34. Patel MR, Ellerton J, Infante JR, Agrawal M, Gordon M, Aljumaily R, et al. Avelumab in metastatic urothelial carcinoma after platinum failure (JAVELIN Solid Tumor): pooled results from two expansion cohorts of an open-label, phase 1 trial. Lancet Oncol. 2018;19(1):51-64.
35. Powles T, O'Donnell PH, Massard C, Arkenau HT, Friedlander TW, Hoimes CJ, et al. Efficacy and Safety of Durvalumab in Locally Advanced or Metastatic Urothelial Carcinoma: Updated Results From a Phase 1/2 Open-label Study. JAMA Oncol. 2017;3(9):e172411.
36. Ganesh K, Stadler ZK, Cercek A, Mendelsohn RB, Shia J, Segal NH, et al. Immunotherapy in colorectal cancer: rationale, challenges and potential. Nat Rev Gastroenterol Hepatol. 2019;16(6):361-75.
37. Fuchs CS, Doi T, Jang RW, Muro K, Satoh T, Machado M, et al. Safety and Efficacy of Pembrolizumab Monotherapy in Patients With Previously Treated Advanced Gastric and Gastroesophageal Junction Cancer: Phase 2 Clinical KEYNOTE-059 Trial. JAMA Oncol. 2018;4(5):e180013.
38. Kole C, Charalampakis N, Tsakatikas S, Vailas M, Moris D, Gkotsis E, et al. Immunotherapy for Hepatocellular Carcinoma: A 2021 Update. Cancers (Basel). 2020;12(10).
39. Ai L, Xu A, Xu J. Roles of PD-1/PD-L1 Pathway: Signaling, Cancer, and Beyond. Adv Exp Med Biol. 2020;1248:33-59.
40. Kawakami Y, Ohta S, Sayem MA, Tsukamoto N, Yaguchi T. Immune-resistant mechanisms in cancer immunotherapy. Int J Clin Oncol. 2020;25(5):810-7.
41. Antonios JP, Soto H, Everson RG, Moughon D, Orpilla JR, Shin NP, et al. Immunosuppressive tumor-infiltrating myeloid cells mediate adaptive immune resistance via a PD-1/PD-L1 mechanism in glioblastoma. Neuro Oncol. 2017;19(6):796-807.
42. Bullock BL, Kimball AK, Poczobutt JM, Neuwelt AJ, Li HY, Johnson AM, et al. Tumor-intrinsic response to IFNγ shapes the tumor microenvironment and anti-PD-1 response in NSCLC. Life Sci Alliance. 2019;2(3).
43. Gainor JF, Shaw AT, Sequist LV, Fu X, Azzoli CG, Piotrowska Z, et al. EGFR Mutations and ALK Rearrangements Are Associated with Low Response Rates to PD-1 Pathway Blockade in Non-Small Cell Lung Cancer: A Retrospective Analysis. Clin Cancer Res. 2016;22(18):4585-93.
44. Bai J, Gao Z, Li X, Dong L, Han W, Nie J. Regulation of PD-1/PD-L1 pathway and resistance to PD-1/PD-L1 blockade. Oncotarget. 2017;8(66):110693-707.
45. Ribas A, Shin DS, Zaretsky J, Frederiksen J, Cornish A, Avramis E, et al. PD-1 Blockade Expands Intratumoral Memory T Cells. Cancer Immunol Res. 2016;4(3):194-203.

46. Peng DH, Rodriguez BL, Diao L, Chen L, Wang J, Byers LA, et al. Collagen promotes anti-PD-1/PD-L1 resistance in cancer through LAIR1-dependent CD8. Nat Commun. 2020;11(1):4520.
47. Huang AC, Postow MA, Orlowski RJ, Mick R, Bengsch B, Manne S, et al. T-cell invigoration to tumour burden ratio associated with anti-PD-1 response. Nature. 2017;545(7652):60-5.
48. Koyama S, Akbay EA, Li YY, Herter-Sprie GS, Buczkowski KA, Richards WG, et al. Adaptive resistance to therapeutic PD-1 blockade is associated with upregulation of alternative immune checkpoints. Nat Commun. 2016;7:10501.
49. Pathak R, Pharaon RR, Mohanty A, Villaflor VM, Salgia R, Massarelli E. Acquired Resistance to PD-1/PD-L1 Blockade in Lung Cancer: Mechanisms and Patterns of Failure. Cancers (Basel). 2020;12(12).
50. Seliger B. Basis of PD1/PD-L1 Therapies. J Clin Med. 2019;8(12).
51. Carbognin L, Pilotto S, Milella M, Vaccaro V, Brunelli M, Caliò A, et al. Differential Activity of Nivolumab, Pembrolizumab and MPDL3280A according to the Tumor Expression of Programmed Death-Ligand-1 (PD-L1): Sensitivity Analysis of Trials in Melanoma, Lung and Genitourinary Cancers. PLoS One. 2015;10(6):e0130142.
52. Shimizu A, Kaira K, Okubo Y, Utsumi D, Yasuda M, Asao T, et al. Positive PD-L1 Expression Predicts Worse Outcome in Cutaneous Angiosarcoma. J Glob Oncol. 2017;3(4):360-9.
53. Incorvaia L, Fanale D, Badalamenti G, Barraco N, Bono M, Corsini LR, et al. Programmed Death Ligand 1 (PD-L1) as a Predictive Biomarker for Pembrolizumab Therapy in Patients with Advanced Non-Small-Cell Lung Cancer (NSCLC). Adv Ther. 2019;36(10):2600-17.
54. Patel SP, Kurzrock R. PD-L1 Expression as a Predictive Biomarker in Cancer Immunotherapy. Mol Cancer Ther. 2015;14(4):847-56.
55. Cho J, Lee J, Bang H, Kim ST, Park SH, An JY, et al. Programmed cell death-ligand 1 expression predicts survival in patients with gastric carcinoma with microsatellite instability. Oncotarget. 2017;8(8):13320-8.
56. Gibney GT, Weiner LM, Atkins MB. Predictive biomarkers for checkpoint inhibitor-based immunotherapy. Lancet Oncol. 2016;17(12):e542-e51.
57. Okada H, Weller M, Huang R, Finocchiaro G, Gilbert MR, Wick W, et al. Immunotherapy response assessment in neuro-oncology: a report of the RANO working group. Lancet Oncol. 2015;16(15):e534-e42.
58. Bellmunt J, de Wit R, Vaughn DJ, Fradet Y, Lee JL, Fong L, et al. Pembrolizumab as Second-Line Therapy for Advanced Urothelial Carcinoma. N Engl J Med. 2017;376(11):1015-26.
59. Burtness B, Harrington KJ, Greil R, Soulières D, Tahara M, de Castro G, et al. Pembrolizumab alone or with chemotherapy versus cetuximab with chemotherapy for recurrent or metastatic squamous cell carcinoma of the head and neck (KEYNOTE-048): a randomised, open-label, phase 3 study. Lancet. 2019;394(10212):1915-28.
60. Massard C, Gordon MS, Sharma S, Rafii S, Wainberg ZA, Luke J, et al. Safety and Efficacy of Durvalumab (MEDI4736), an Anti-Programmed Cell Death Ligand-1 Immune Checkpoint Inhibitor, in Patients With Advanced Urothelial Bladder Cancer. J Clin Oncol. 2016;34(26):3119-25.
61. Apolo AB, Infante JR, Balmanoukian A, Patel MR, Wang D, Kelly K, et al. Avelumab, an Anti-Programmed Death-Ligand 1 Antibody, In Patients With Refractory Metastatic Urothelial Carcinoma: Results From a Multicenter, Phase Ib Study. J Clin Oncol. 2017;35(19):2117-24.
62. Munari E, Mariotti FR, Quatrini L, Bertoglio P, Tumino N, Vacca P, et al. PD-1/PD-L1 in Cancer: Pathophysiological, Diagnostic and Therapeutic Aspects. Int J Mol Sci. 2021;22(10).
63. Doroshow DB, Bhalla S, Beasley MB, Sholl LM, Kerr KM, Gnjatic S, et al. PD-L1 as a biomarker of response to immune-checkpoint inhibitors. Nat Rev Clin Oncol. 2021;18(6):345-62.
64. Madore J, Strbenac D, Vilain R, Menzies AM, Yang JY, Thompson JF, et al. PD-L1 Negative Status is Associated with Lower Mutation Burden, Differential Expression of Immune-Related Genes, and Worse Survival in Stage III Melanoma. Clin Cancer Res. 2016;22(15):3915-23.
65. Hellmann MD, Callahan MK, Awad MM, Calvo E, Ascierto PA, Atmaca A, et al. Tumor Mutational Burden and Efficacy of Nivolumab Monotherapy and in Combination with Ipilimumab in Small-Cell Lung Cancer. Cancer Cell. 2018;33(5):853-61.e4.
66. Borghaei H, Paz-Ares L, Horn L, Spigel DR, Steins M, Ready NE, et al. Nivolumab versus Docetaxel in Advanced Nonsquamous Non-Small-Cell Lung Cancer. N Engl J Med. 2015;373(17):1627-39.
67. Benyamine A, Loncle C, Foucher E, Blazquez JL, Castanier C, Chrétien AS, et al. BTN3A is a prognosis marker and a promising target for Vγ9Vδ2 T cells based-immunotherapy in pancreatic ductal adenocarcinoma (PDAC). Oncoimmunology. 2017;7(1):e1372080.

68. Di Marco Barros R, Roberts NA, Dart RJ, Vantourout P, Jandke A, Nussbaumer O, et al. Epithelia Use Butyrophilin-like Molecules to Shape Organ-Specific γδ T Cell Compartments. Cell. 2016;167(1):203-18.e17.
69. Vlachos IS, Kostoulas N, Vergoulis T, Georgakilas G, Reczko M, Maragkakis M, et al. DIANA miRPath v.2.0: investigating the combinatorial effect of microRNAs in pathways. Nucleic Acids Res. 2012;40(Web Server issue):W498-504.
70. Du Y, Peng Q, Cheng D, Pan T, Sun W, Wang H, et al. Cancer cell-expressed BTNL2 facilitates tumour immune escape via engagement with IL-17A-producing γδ T cells. Nat Commun. 2022;13(1):231.
71. Bian B, Fanale D, Dusetti N, Roque J, Pastor S, Chretien AS, et al. Prognostic significance of circulating PD-1, PD-L1, pan-BTN3As, BTN3A1 and BTLA in patients with pancreatic adenocarcinoma. Oncoimmunology. 2019;8(4):e1561120.
72. Ding L, Lu S, Li Y. Regulation of PD-1/PD-L1 Pathway in Cancer by Noncoding RNAs. Pathol Oncol Res. 2020;26(2):651-63.
73. Braicu C, Zimta AA, Harangus A, Iurca I, Irimie A, Coza O, et al. The Function of Non-Coding RNAs in Lung Cancer Tumorigenesis. Cancers (Basel). 2019;11(5).
74. Iqbal MA, Arora S, Prakasam G, Calin GA, Syed MA. MicroRNA in lung cancer: role, mechanisms, pathways and therapeutic relevance. Mol Aspects Med. 2019;70:3-20.
75. Bayraktar R, Van Roosbroeck K. miR-155 in cancer drug resistance and as target for miRNA-based therapeutics. Cancer Metastasis Rev. 2018;37(1):33-44.
76. Mashima R. Physiological roles of miR-155. Immunology. 2015;145(3):323-33.
77. Li X, Zhao H, Zhou X, Song L. Inhibition of lactate dehydrogenase A by microRNA-34a resensitizes colon cancer cells to 5-fluorouracil. Mol Med Rep. 2015;11(1):577-82.
78. Cortez MA, Ivan C, Valdecanas D, Wang X, Peltier HJ, Ye Y, et al. PDL1 Regulation by p53 via miR-34. J Natl Cancer Inst. 2016;108(1).
79. Kang M, Li Y, Zhao Y, He S, Shi J. miR-33a inhibits cell proliferation and invasion by targeting CAND1 in lung cancer. Clin Transl Oncol. 2018;20(4):457-66.
80. Boldrini L, Giordano M, Niccoli C, Melfi F, Lucchi M, Mussi A, et al. Role of microRNA-33a in regulating the expression of PD-1 in lung adenocarcinoma. Cancer Cell Int. 2017;17:105.
81. Pfeffer SR, Yang CH, Pfeffer LM. The Role of miR-21 in Cancer. Drug Dev Res. 2015;76(6):270-7.
82. Zheng X, Dong L, Wang K, Zou H, Zhao S, Wang Y, et al. MiR-21 Participates in the PD-1/PD-L1 Pathway-Mediated Imbalance of Th17/Treg Cells in Patients After Gastric Cancer Resection. Ann Surg Oncol. 2019;26(3):884-93.
83. Fujita Y, Yagishita S, Hagiwara K, Yoshioka Y, Kosaka N, Takeshita F, et al. The clinical relevance of the miR-197/CKS1B/STAT3-mediated PD-L1 network in chemoresistant non-small-cell lung cancer. Mol Ther. 2015;23(4):717-27.
84. Tang D, Zhao D, Wu Y, Yao R, Zhou L, Lu L, et al. The miR-3127-5p/p-STAT3 axis up-regulates PD-L1 inducing chemoresistance in non-small-cell lung cancer. J Cell Mol Med. 2018;22(8):3847-56.
85. Xi J, Huang Q, Wang L, Ma X, Deng Q, Kumar M, et al. miR-21 depletion in macrophages promotes tumoricidal polarization and enhances PD-1 immunotherapy. Oncogene. 2018;37(23):3151-65.
86. Zhu J, Chen L, Zou L, Yang P, Wu R, Mao Y, et al. MiR-20b, -21, and -130b inhibit PTEN expression resulting in B7-H1 over-expression in advanced colorectal cancer. Hum Immunol. 2014;75(4):348-53.
87. Siravegna G, Marsoni S, Siena S, Bardelli A. Integrating liquid biopsies into the management of cancer. Nat Rev Clin Oncol. 2017;14(9):531-48.
88. Yin Z, Yu M, Ma T, Zhang C, Huang S, Karimzadeh MR, et al. Mechanisms underlying low-clinical responses to PD-1/PD-L1 blocking antibodies in immunotherapy of cancer: a key role of exosomal PD-L1. J Immunother Cancer. 2021;9(1).
89. Greening DW, Gopal SK, Xu R, Simpson RJ, Chen W. Exosomes and their roles in immune regulation and cancer. Semin Cell Dev Biol. 2015;40:72-81.
90. Yi M, Xu L, Jiao Y, Luo S, Li A, Wu K. The role of cancer-derived microRNAs in cancer immune escape. J Hematol Oncol. 2020;13(1):25.
91. Sun Z, Shi K, Yang S, Liu J, Zhou Q, Wang G, et al. Effect of exosomal miRNA on cancer biology and clinical applications. Mol Cancer. 2018;17(1):147.
92. Hofman P, Heeke S, Alix-Panabières C, Pantel K. Liquid biopsy in the era of immuno-oncology: is it ready for prime-time use for cancer patients? Ann Oncol. 2019;30(9):1448-59.
93. Yang Y, Li CW, Chan LC, Wei Y, Hsu JM, Xia W, et al. Exosomal PD-L1 harbors active defense function to suppress T cell killing of breast cancer cells and promote tumor growth. Cell Res. 2018;28(8):862-4.

94. Theodoraki MN, Yerneni SS, Hoffmann TK, Gooding WE, Whiteside TL. Clinical Significance of PD-L1. Clin Cancer Res. 2018;24(4):896-905.
95. Chen G, Huang AC, Zhang W, Zhang G, Wu M, Xu W, et al. Exosomal PD-L1 contributes to immunosuppression and is associated with anti-PD-1 response. Nature. 2018;560(7718):382-6.
96. Molga-Magusiak M, Rzepakowska A, Żurek M, Kotuła I, Demkow U, Niemczyk K. Prognostic and predictive role of soluble programmed death ligand-1 in head and neck cancer. Braz J Otorhinolaryngol. 2023;89(3):417-24.
97. Li HB, Yang ZH, Guo QQ. Immune checkpoint inhibition for pancreatic ductal adenocarcinoma: limitations and prospects: a systematic review. Cell Commun Signal. 2021;19(1):117.
98. Zheng Z, Bu Z, Liu X, Zhang L, Li Z, Wu A, et al. Level of circulating PD-L1 expression in patients with advanced gastric cancer and its clinical implications. Chin J Cancer Res. 2014;26(1):104-11.
99. Sorensen SF, Demuth C, Weber B, Sorensen BS, Meldgaard P. Increase in soluble PD-1 is associated with prolonged survival in patients with advanced EGFR-mutated non-small cell lung cancer treated with erlotinib. Lung Cancer. 2016;100:77-84.
100. Tiako Meyo M, Jouinot A, Giroux-Leprieur E, Fabre E, Wislez M, Alifano M, et al. Predictive Value of Soluble PD-1, PD-L1, VEGFA, CD40 Ligand and CD44 for Nivolumab Therapy in Advanced Non-Small Cell Lung Cancer: A Case-Control Study. Cancers (Basel). 2020;12(2).
101. Chang B, Huang T, Wei H, Shen L, Zhu D, He W, et al. The correlation and prognostic value of serum levels of soluble programmed death protein 1 (sPD-1) and soluble programmed death-ligand 1 (sPD-L1) in patients with hepatocellular carcinoma. Cancer Immunol Immunother. 2019;68(3):353-63.
102. Tominaga T, Akiyoshi T, Yamamoto N, Taguchi S, Mori S, Nagasaki T, et al. Clinical significance of soluble programmed cell death-1 and soluble programmed cell death-ligand 1 in patients with locally advanced rectal cancer treated with neoadjuvant chemoradiotherapy. PLoS One. 2019;14(2):e0212978.
103. Murakami S, Shibaki R, Matsumoto Y, Yoshida T, Goto Y, Kanda S, et al. Association between serum level soluble programmed cell death ligand 1 and prognosis in patients with non-small cell lung cancer treated with anti-PD-1 antibody. Thorac Cancer. 2020;11(12):3585-95.
104. Larrinaga G, Solano-Iturri JD, Errarte P, Unda M, Loizaga-Iriarte A, Pérez-Fernández A, et al. Soluble PD-L1 Is an Independent Prognostic Factor in Clear Cell Renal Cell Carcinoma. Cancers (Basel). 2021;13(4).
105. Vikerfors A, Davidsson S, Frey J, Jerlström T, Carlsson J. Soluble PD-L1 in Serum and Urine in Urinary Bladder Cancer Patients. Cancers (Basel). 2021;13(22).
106. Fu R, Jing CQ, Li XR, Tan ZF, Li HJ. Prognostic Significance of Serum PD-L1 Level in Patients with Locally Advanced or Metastatic Esophageal Squamous Cell Carcinoma Treated with Combination Cytotoxic Chemotherapy. Cancer Manag Res. 2021;13:4935-46.
107. Ding XC, Wang LL, Zhu YF, Li YD, Nie SL, Yang J, et al. The Change of Soluble Programmed Cell Death-Ligand 1 in Glioma Patients Receiving Radiotherapy and Its Impact on Clinical Outcomes. Front Immunol. 2020;11:580335.
108. Mocan T, Ilies M, Nenu I, Craciun R, Horhat A, Susa R, et al. Serum levels of soluble programmed death-ligand 1 (sPD-L1): A possible biomarker in predicting post-treatment outcomes in patients with early hepatocellular carcinoma. Int Immunopharmacol. 2021;94:107467.
109. Zhou J, Mahoney KM, Giobbie-Hurder A, Zhao F, Lee S, Liao X, et al. Soluble PD-L1 as a Biomarker in Malignant Melanoma Treated with Checkpoint Blockade. Cancer Immunol Res. 2017;5(6):480-92.
110. Cheng Y, Wang C, Wang Y, Dai L. Soluble PD-L1 as a predictive biomarker in lung cancer: a systematic review and meta-analysis. Future Oncol. 2022;18(2):261-73.
111. Fromm B, Billipp T, Peck LE, Johansen M, Tarver JE, King BL, et al. A Uniform System for the Annotation of Vertebrate microRNA Genes and the Evolution of the Human microRNAome. Annu Rev Genet. 2015;49:213-42.
112. Kozomara A, Griffiths-Jones S. miRBase: integrating microRNA annotation and deep-sequencing data. Nucleic Acids Res. 2011;39(Database issue):D152-7.
113. Kanehisa M, Goto S, Sato Y, Furumichi M, Tanabe M. KEGG for integration and interpretation of large-scale molecular data sets. Nucleic Acids Res. 2012;40(Database issue):D109-14.
114. Tsai KK, Daud AI. The Role of Anti-PD-1/PD-L1 Agents in Melanoma: Progress to Date. Drugs. 2015;75(6):563-75.
115. Gong J, Chehrazi-Raffle A, Reddi S, Salgia R. Development of PD-1 and PD-L1 inhibitors as a form of cancer immunotherapy: a comprehensive review of registration trials and future considerations. J Immunother Cancer. 2018;6(1):8.

116. Zavala VA, Kalergis AM. New clinical advances in immunotherapy for the treatment of solid tumours. Immunology. 2015;145(2):182-201.
117. Haslam A, Prasad V. Estimation of the Percentage of US Patients With Cancer Who Are Eligible for and Respond to Checkpoint Inhibitor Immunotherapy Drugs. JAMA Netw Open. 2019;2(5):e192535.
118. Davis AA, Patel VG. The role of PD-L1 expression as a predictive biomarker: an analysis of all US Food and Drug Administration (FDA) approvals of immune checkpoint inhibitors. J Immunother Cancer. 2019;7(1):278.
119. Gu L, Chen M, Guo D, Zhu H, Zhang W, Pan J, et al. PD-L1 and gastric cancer prognosis: A systematic review and meta-analysis. PLoS One. 2017;12(8):e0182692.
120. Ohigashi Y, Sho M, Yamada Y, Tsurui Y, Hamada K, Ikeda N, et al. Clinical significance of programmed death-1 ligand-1 and programmed death-1 ligand-2 expression in human esophageal cancer. Clin Cancer Res. 2005;11(8):2947-53.
121. Chen L, Deng H, Lu M, Xu B, Wang Q, Jiang J, et al. B7-H1 expression associates with tumor invasion and predicts patient's survival in human esophageal cancer. Int J Clin Exp Pathol. 2014;7(9):6015-23.
122. Chen XL, Yuan SX, Chen C, Mao YX, Xu G, Wang XY. [Expression of B7-H1 protein in human pancreatic carcinoma tissues and its clinical significance]. Ai Zheng. 2009;28(12):1328-32.
123. Hamanishi J, Mandai M, Iwasaki M, Okazaki T, Tanaka Y, Yamaguchi K, et al. Programmed cell death 1 ligand 1 and tumor-infiltrating CD8+ T lymphocytes are prognostic factors of human ovarian cancer. Proc Natl Acad Sci U S A. 2007;104(9):3360-5.
124. Schalper KA, Velcheti V, Carvajal D, Wimberly H, Brown J, Pusztai L, et al. In situ tumor PD-L1 mRNA expression is associated with increased TILs and better outcome in breast carcinomas. Clin Cancer Res. 2014;20(10):2773-82.
125. Incorvaia L, Badalamenti G, Rinaldi G, Iovanna JL, Olive D, Swayden M, et al. Can the plasma PD-1 levels predict the presence and efficiency of tumor-infiltrating lymphocytes in patients with metastatic melanoma? Ther Adv Med Oncol. 2019;11:1758835919848872.
126. Incorvaia L, Bronte G, Bazan V, Badalamenti G, Rizzo S, Pantuso G, et al. Beyond evidence-based data: scientific rationale and tumor behavior to drive sequential and personalized therapeutic strategies for the treatment of metastatic renal cell carcinoma. Oncotarget. 2016;7(16):21259-71.
127. Joosten SC, Smits KM, Aarts MJ, Melotte V, Koch A, Tjan-Heijnen VC, et al. Epigenetics in renal cell cancer: mechanisms and clinical applications. Nat Rev Urol. 2018;15(7):430-51.
128. Fan W, Huang J, Xiao H, Liang Z. MicroRNA-22 is downregulated in clear cell renal cell carcinoma, and inhibits cell growth, migration and invasion by targeting PTEN. Mol Med Rep. 2016;13(6):4800-6.
129. Bar N, Dikstein R. miR-22 forms a regulatory loop in PTEN/AKT pathway and modulates signaling kinetics. PLoS One. 2010;5(5):e10859.
130. Gong X, Zhao H, Saar M, Peehl DM, Brooks JD. miR-22 Regulates Invasion, Gene Expression and Predicts Overall Survival in Patients with Clear Cell Renal Cell Carcinoma. Kidney Cancer. 2019;3(2):119-32.
131. Jin L, Li Y, Nie L, He T, Hu J, Liu J, et al. MicroRNA-24-2 is associated with cell proliferation, invasion, migration and apoptosis in renal cell carcinoma. Mol Med Rep. 2017;16(6):9157-64.
132. Quan J, Liu S, Dai K, Jin L, He T, Pan X, et al. MicroRNA-23a/24-2/27a as a potential diagnostic biomarker for cancer: A systematic review and meta-analysis. Mol Clin Oncol. 2018;8(1):159-69.
133. Cui L, Zhou H, Zhao H, Zhou Y, Xu R, Xu X, et al. MicroRNA-99a induces G1-phase cell cycle arrest and suppresses tumorigenicity in renal cell carcinoma. BMC Cancer. 2012;12:546.
134. Oliveira RC, Ivanovic RF, Leite KRM, Viana NI, Pimenta RCA, Junior JP, et al. Expression of micro-RNAs and genes related to angiogenesis in ccRCC and associations with tumor characteristics. BMC Urol. 2017;17(1):113.
135. Khella HW, Bakhet M, Allo G, Jewett MA, Girgis AH, Latif A, et al. miR-192, miR-194 and miR-215: a convergent microRNA network suppressing tumor progression in renal cell carcinoma. Carcinogenesis. 2013;34(10):2231-9.
136. Ran L, Liang J, Deng X, Wu J. miRNAs in Prediction of Prognosis in Clear Cell Renal Cell Carcinoma. Biomed Res Int. 2017;2017:4832931.
137. Das F, Dey N, Bera A, Kasinath BS, Ghosh-Choudhury N, Choudhury GG. MicroRNA-214 Reduces Insulin-like Growth Factor-1 (IGF-1) Receptor Expression and Downstream mTORC1 Signaling in Renal Carcinoma Cells. J Biol Chem. 2016;291(28):14662-76.

138. Xu H, Wu S, Shen X, Shi Z, Wu D, Yuan Y, et al. Methylation-mediated miR-214 regulates proliferation and drug sensitivity of renal cell carcinoma cells through targeting LIVIN. J Cell Mol Med. 2020;24(11):6410-25.
139. Wang K, Chen X, Zhan Y, Jiang W, Liu X, Wang X, et al. miR-335 inhibits the proliferation and invasion of clear cell renal cell carcinoma cells through direct suppression of BCL-W. Tumour Biol. 2015;36(9):6875-82.
140. Saini S, Yamamura S, Majid S, Shahryari V, Hirata H, Tanaka Y, et al. MicroRNA-708 induces apoptosis and suppresses tumorigenicity in renal cancer cells. Cancer Res. 2011;71(19):6208-19.
141. Dragomir M, Chen B, Fu X, Calin GA. Key questions about the checkpoint blockade-are microRNAs an answer? Cancer Biol Med. 2018;15(2):103-15.
142. Chen L, Gibbons DL, Goswami S, Cortez MA, Ahn YH, Byers LA, et al. Metastasis is regulated via microRNA-200/ZEB1 axis control of tumour cell PD-L1 expression and intratumoral immunosuppression. Nat Commun. 2014;5:5241.
143. Raimondi A, Randon G, Sepe P, Claps M, Verzoni E, de Braud F, et al. The Evaluation of Response to Immunotherapy in Metastatic Renal Cell Carcinoma: Open Challenges in the Clinical Practice. Int J Mol Sci. 2019;20(17).
144. George S, Motzer RJ, Hammers HJ, Redman BG, Kuzel TM, Tykodi SS, et al. Safety and Efficacy of Nivolumab in Patients With Metastatic Renal Cell Carcinoma Treated Beyond Progression: A Subgroup Analysis of a Randomized Clinical Trial. JAMA Oncol. 2016;2(9):1179-86.
145. Trestini I, Caldart A, Dodi A, Avancini A, Tregnago D, Sartori G, et al. Body composition as a modulator of response to immunotherapy in lung cancer: time to deal with it. ESMO Open. 2021;6(2):100095.
146. Wang Z, Aguilar EG, Luna JI, Dunai C, Khuat LT, Le CT, et al. Paradoxical effects of obesity on T cell function during tumor progression and PD-1 checkpoint blockade. Nat Med. 2019;25(1):141-51.
147. Naylor C, Petri WA. Leptin Regulation of Immune Responses. Trends Mol Med. 2016;22(2):88-98.
148. Saucillo DC, Gerriets VA, Sheng J, Rathmell JC, Maciver NJ. Leptin metabolically licenses T cells for activation to link nutrition and immunity. J Immunol. 2014;192(1):136-44.